



Detrital Zircon U–Pb Geochronology and Provenance of Bayan Obo Group, Northern Margin of North China Craton: New Implications for the Position of NCC in Rodinia

LI Changhai^{1,2}, LIU Zhenghong^{1,*}, XU Zhongyuan¹, DONG Xiaojie¹, LI Pengchuan¹, SHI Qiang¹ and WANG Shijie¹

¹ College of Earth Sciences, Jilin University, Changchun 130001, China

² Key Laboratory of Mineral Resources Evaluation in Northeast Asia, Ministry of Natural Resources, Changchun 130026, China

Abstract: The paleoposition of North China Craton in Rodinia has long been in controversial. This paper mainly focuses on the U–Pb geochronological studies of detrital zircons obtained from Bayan Obo Group exposed in the Shangdu area, Inner Mongolia, aiming to provide more information for interpreting this problem. Based on the acquired data, this paper comes to the following conclusions. Firstly, the depositional age of Bayan Obo Group might be from Meso- to Neoproterozoic according to the zircons U–Pb dating results. The lower succession of this group, namely Dulahala and Jianshan formations deposited between 1800 and 1650 Ma. The Halahuogete and Bilute formations deposited between 1500 and 1350 Ma. For Baiyinbaolage and Hujertu formations, their depositional age was 1250–900 Ma. Secondly, for the provenance of Bayan Obo Group, this paper believes detrital zircons with age of 2.51–2.71 Ga and 2.00–2.48 Ga were from Guyang, Xi Ulanbulang and Zhuozhi area; the Khondalite Belt provided detrital zircons with age of 1.95–1.80 Ga; zircons with age of 1.60–1.75 Ga might come from granitic rocks in Miyun Area. The magmatism after 1.60 Ga was rarely recorded in the NCC, therefore those zircons with ages younger than 1.60 Ga might come from outside of NCC. The magmatism with the same age existed in Baltic, Amazonia and Laurentia. Based on previous paleomagnetic researches, this paper proposes that NCC might receive detritus from Baltic during 1560–1350 Ma and had affinity with Laurentia and Amazonia at ~0.9 Ga in Rodinia. Baltic, Amazonia and Laurentia might be potential provenances for non–NCC detritus in Bayan Obo Group.

Key words: North China Craton, Precambria, Bayan Obo Group, detrital zircons, Rodinia

Citation: Li et al., 2019. Detrital Zircon U–Pb Geochronology and Provenance of Bayan Obo Group, Northern Margin of North China Craton: New Implications for the Position of NCC in Rodinia. *Acta Geologica Sinica (English Edition)*, 93(5): 1397–1416. DOI: 10.1111/1755-6724.14354

1 Introduction

The collision, assembly and break-up of continents represent special and critical periods in the history of Earth. The configuration and assembling way of supercontinents have been hot topics among geologists in the past few decades (Piper, 1982; Rogers, 1996; Smethurst et al., 1998; Åhäll et al., 1998; Piper, 2000; CorreaGomes et al., 2000; Dalziel et al., 2000; Rogers et al., 2002; Evans et al., 2011; Zhang et al., 2012; Evans, 2013; Wen et al., 2018). After the SWEAT hypothesis for Rodinia reconstruction was firstly put forward in last century (Dalziel, 1991; Moores, 1991; Hoffman, 1991), many other geologists also came up with different Rodinia configuration hypothesis based on geological and paleomagnetic evidences, such as AUSWUS (Karlstrom et al., 1999), AUSMEX (Wingate et al., 2002) and SAMBA (Johansson, 2009). SWAET, AUSWUS and AUSMEX models connected Australia to the north-western, western and southern part of Laurentia, SAMBA assured the proximity between Amazonia and Baltic. All in all,

positioning Laurentia in the central part of Rodinia was the similarity for these configuration models (Li et al., 2008). However, these models seldom discussed the paleoposition of NCC in Rodinia. Because ~1.0 Ga magmatism is scarcely reported in NCC, whether and how it was involved in the evolution of Rodinia are still unclear enough.

North China Craton has been gradually becoming a popular studying area of precambrian geology. The ~1.95 Ga Khondalite Belt in western block and the ~1.85 Ga Trans–North–China–Orogen witnessed the involvement of NCC in Columbia (Zhao et al., 1999a; Zhao et al., 1999b; Zhao et al., 2000a; Zhao et al., 2000b; Rogers et al., 2002; Zhao et al., 2003; Zhai et al., 2003; Kusky et al., 2009; Santosh, 2010). Based on geological and paleomagnetic facts, NCC might connect with Siberia, Baltic, Laurentia and India in Columbia (Rogers et al., 2002; Zhao et al., 2003; Liu et al., 2014; Xu et al., 2014; Liu et al., 2018). The separation of NCC from Columbia might commence roughly at 1400Ma and ended at 1.32–1.30 Ga (Zhang et al., 2009; Zhang et al., 2012; Zhang et al., 2017).

Rodinia was assembled by the ~1.0 Ga Grenville orogenesis, the position of NCC in Rodinia has been

* Corresponding author. E-mail: zhliu@jlu.edu.cn

tentatively discussed from the perspective of geology and paleomagnetism. Given NCC and Laurentia showed similar APWPs during 1200–700 Ma (Zhang et al., 2006) and the similarities between Mesoproterozoic strata exposed in NCC and Siberia, NCC might be adjacent to Siberia and the northwestern part of Laurentia in Rodinia (Li et al., 1996; Li et al., 2008). According to the studies on provenance of Neoproterozoic strata in the north margin of NCC, Liu C H et al. (2017) proposed proximity between Baltic and NCC in Rodinia. However, relevant discussions about the position of NCC in Rodinia are still limited, more data are needed for a better understanding towards this question.

Zircons have been extensively applied in the geochronological studies for its stability and resistance (Won Kim et al., 2019; Pulsipher et al., 2019). Detrital zircons have been gradually becoming a useful tool for determining the maximum depositional age and provenance of clastic strata, geochronological studies on detrital zircons will also have great significance in interpreting the proximity among different blocks. In the north margin of NCC lies Meso- to Neoproterozoic strata called Bayan Obo Group, this paper launches studies on U–Pb geochronology of detrital zircons from this group and illustrates evolving history of NCC during the transition from Columbia to Rodinia. Furthermore, potential proximity among NCC, Baltic, Amazonia and Laurentia from 1.5 Ga to 0.9 Ga is also discussed in this paper.

2 Geological Background

As one of the oldest cratons globally (Zhai, 2013; Zhai, 2014), NCC was assembled by the collision between eastern and western part at ~1.85 Ga (Zhao et al., 2000b; Zhao et al., 2004; Zhao et al., 2008; Zhao et al., 2011; Zhao et al., 2012) (Fig. 1). Then it went through broad extensional period from ~1.85 Ga, the representative magmatism included the intrusion of ~1.78 Ga mafic dykes, Xiong'er volcanic succession (Peng et al., 2007; Peng, 2015), 1.72–1.62 Ga non-orogenic magmatism, large igneous province at 1.32 Ga as well as mafic dykes at 900 Ma (Lu et al., 2002; Zhai et al., 2003; Zhang et al., 2007; Zhai et al., 2011a; Zhai, 2011b; Zhai et al., 2015). All in all, NCC was in a post-orogenic extensional tectonic setting during 1.7–0.9 Ga, when the mantle went through a secular cooling process which was one of main characteristics during the *Earth's Middle Age* (Hawkesworth et al., 2014).

The constant rifting led to the formation of Yanliao (Lu et al., 2008), Zha'ertai–Bayan Obo (Li et al., 2013; Liu et al., 2014; Zhong et al., 2015; Liu et al., 2018) and Xiong'er rift zone (Zhao et al., 2002; Zhao et al., 2004b) in the eastern, northern and southern part of NCC respectively. In Yanliao rift zone, the strata is divided into Changcheng, Jixian and Qingbaikou system from lower to upper. According to the latest geochronological data, the lower boundary of Changcheng system was constrained at 1650 Ma, ~150 Ma younger than the conventional 1800 Ma (Li et al., 2013). But this age might only represent the sedimentary age in Miyun area, the actual lower boundary

of Changcheng system might be older (Qiao et al., 2014). More and more precise dating results of volcanic interlayers provided better constrains on the sedimentary age of the strata in Yanliao rift zone, such as K-rich volcanic rocks of 1683 ± 67 Ma and 1641 ± 4 Ma from Tuanshanzi Formation (Zhang et al., 2013), volcanic rocks of ~1625 Ma from Dahongyu Formation; tuff of ~1560 Ma from Gaoyuzhuang Formation (Li et al., 2010), bentonite of ~1485 Ma and ~1440 Ma from Wumishan and Tieling Formation respectively (Li et al., 2014); bentonite of 1368–1380 Ma from Xiamaling Formation (Su et al., 2010). Based on the above data, Li et al. (2013) proposed that the lower boundary age of Jixian system should be set at 1600 Ma, a new defined Awaiting System was from 1400 Ma to 1000 Ma (Gao et al., 2011; Li et al., 2013). Meanwhile, the missing of sediment from 1320 Ma to 900 Ma might represent the overall uplift in the Yanliao rift zone (Zhang et al., 2017).

The strata in Langshan–Zha'ertai–Bayan Obo rift zone includes Zha'ertai, Bayan Obo, Huade and Langshan Group. The Zha'ertai Group is mainly composed of epimetamorphic sedimentary rocks, including metamorphic conglomerate, conglomerate-bearing feldspar quartz sandstone, quartzite, dolomite, phyllite and carbonaceous phyllite (Li et al., 2007; Qiao et al., 1991). From the bottom to top, the Zha'ertai Group is divided into the Shujigou, Zenglongchang, Agulugou and Liuhongwan Formation. U–Pb ages of zircons from intermediate–basic volcanic interlayer in Shujigou Formation was 1743 ± 7 Ma (Li et al., 2007), indicating Zha'ertai Group should deposit after that. The ages of detrital zircons in this formation exhibit two clusters at 1.8–1.9 Ga and 2.5 Ga (Gong et al., 2016). Based on the lithological similarity, the Zha'ertai Group may be comparable with Changcheng system in Yanliao rift zone (Gong et al., 2016). However, Liu et al. (2018) suggested that Zha'ertai Group was in an intracratonic position and mainly received sediments older than 1.7 Ga from inner NCC, causing this group might show two age peaks at ~1.85 Ga and ~2.5 Ga even in Neoproterozoic, therefore it might be inappropriate to make the whole Zha'ertai Group equivalent to Changcheng System. Located in the eastern side of the Zha'ertai Group, Huade Group is a set of epimetamorphic or unmetamorphic sedimentary rocks mainly consisting of sandstone, wacke, feldspathic sandstone, mudstone and limestone, some of which have undergone low-grade metamorphism to become quartzite, schist, slate, diopside and marble (Hu et al., 2009). The detrital zircons in the Huade Group defined several age peaks, such as 2530 Ma, 1837 Ma, 1718 Ma, 1575 Ma, 1508 Ma and 1360 Ma, the Sanxiatian Formation on the top of Huade Group deposited simultaneously with Baiyinbaolage Formation of Bayan Obo Group, Liuhongwan Formation of Zha'ertai Group and Xiamaling Formation in Yanliao Rift Zone (Liu et al., 2018). The Langshan Group is in the west of Zha'ertai Group. From bottom to top, the Langshan Group consists of four formations, mainly made up of two mica quartz schist, hornblende marble, metamorphic sandstone, mica quartz schist, limestone and carbonaceous sericite quartz phyllite. The youngest

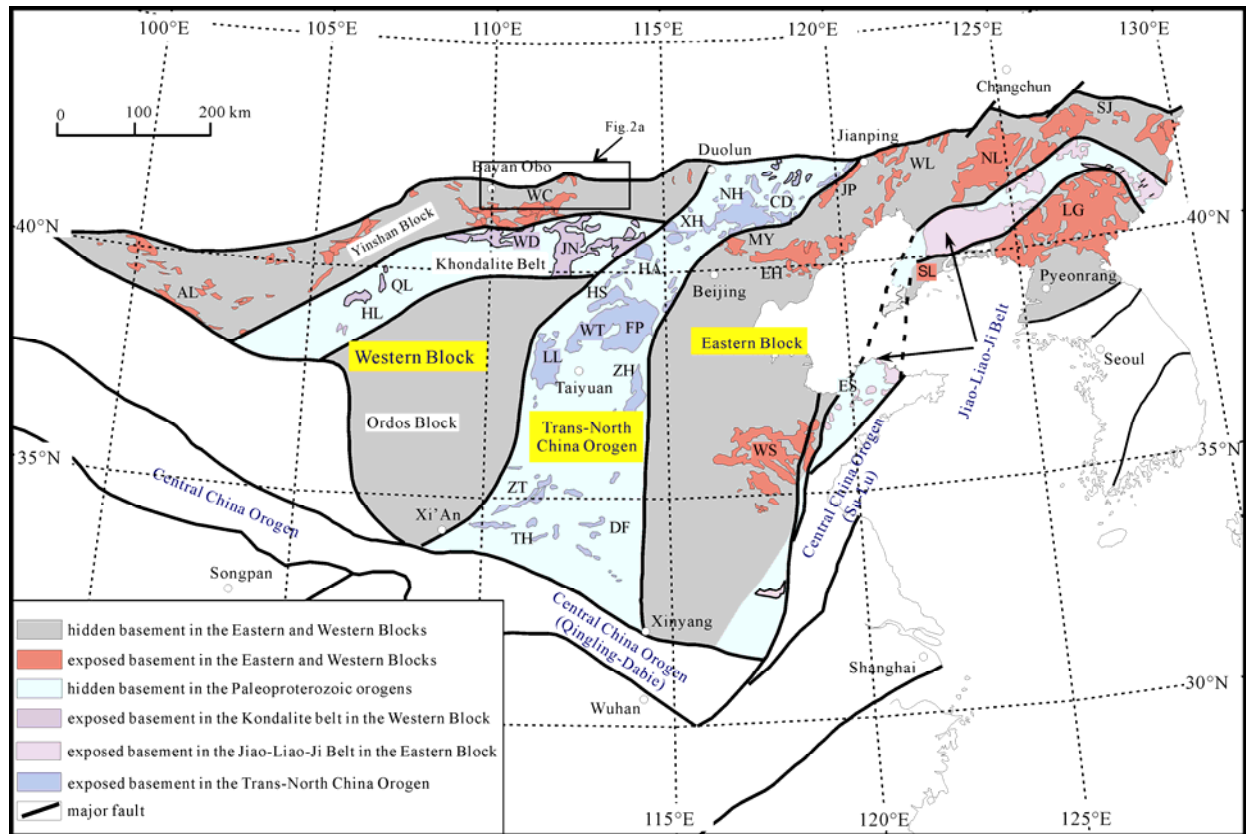


Fig. 1. The Precambrian tectonic divisions of NCC (after Zhao et al., 2006; Zhao et al., 2012).

detrital zircons in metamorphic sedimentary rocks show an age peak at 1187–810 Ma (Hu et al., 2014). Based on the ~804 Ma and ~817 Ma metamorphic acid volcanic rocks in this strata, Langshan Group was believed to be Neoproterozoic sediments (Hu et al., 2015).

The Bayan Obo Group in the studied area can be divided into the Dulahala (Chd), Jianshan (Chj), Halahuogete (Jxh), Bilute (Jxb), Baiyingbaolage (Qnby) and Hujiertu Formation (Qnhj) from bottom to top (Fig. 2). The Dulahala Formation was dominated by clastic rocks, mainly composed of metamorphic pebble-bearing quartz sandstone, metamorphic sandstone and so on. The Jianshan Formation was composed of sericite phyllite and metamorphic coarse sandstone, metamorphic feldsparitic quartz sandstone, with development of cleavage and foliation. The Halahuogete Formation was a set of glutenite, metamorphic conglomerate, dark gray quartz marble and grayish fine-grained limestone. The lithology of the Bilute Formation was mainly sericite phyllite, which was a weak layer in the Bayan Obo Group and had suffered strong deformation. The lithology of Baiyingbaolage Formation was quartzite and meta-quartzite. The lithology and thickness of this formation were stable, therefore, it can serve as a marker layer for regional strata comparison. Hujiertu Formation mainly composed of limestone, sericite slate, silty slate and epidote-chlorite-actinolite schist. Overall, Bayan Obo Group is a set of epimetamorphic strata and has undergone low-grade metamorphism.

3 Samples and Methods

3.1 Sample descriptions

The samples were mainly collected in Shangdu area, Wulanchabu City, Inner Mongolia (Fig. 3, Fig. 4). Sample JN2013–1 was collected from the Dulahala Formation near Banbanshi (Position: N41°36'33", E 113°19'10"). The sample is fine grained meta-quartz sandstone and consists of 95% quartz and 5% cement composed by sericite (Fig. 5a). Sample JN2013–2, sericite phyllite, was collected from the lower part of Jianshan Formation near Banbanshi (Position: N41°36'47", E113°18'45"). The main mineral is sericite, with a content of about 55%; quartz with a content of about 45% (Fig. 5b).

Sample JN2013–3 was collected from Halahuogete Formation, also near Banbanshi (Position: N41°37'35", E113°18'08"), which is a pebble-bearing meta-coarse grained quartz sandstone. The sample is mainly composed by quartz (90%). The cement is almost sericite and its content is about 10% (Fig. 5c).

Sample JN2013–5 was collected from Bilute Formation, and the sampling position was in the north of the Banbanshi (Position: N41°40'18", E113°18'01"). The outcrop is carbonaceous sericite phyllite, the main mineral is sericite with size less than 0.025 mm and its content is about 95%, the rest are quartz with a content of about 5% (Fig. 5d).

Sample JN2013–6 was collected from the Baiyingbaolage Formation, about 1 km north of Xijingzi

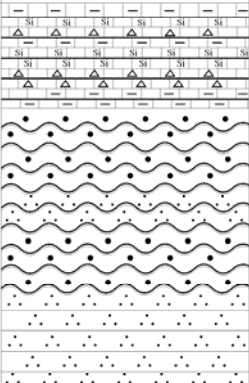
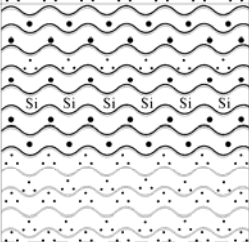
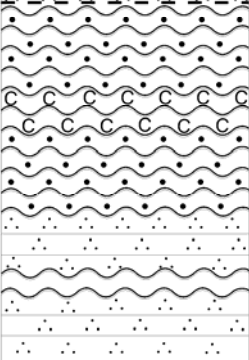
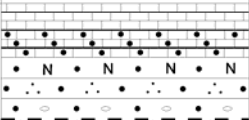
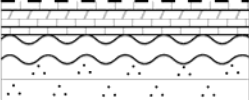
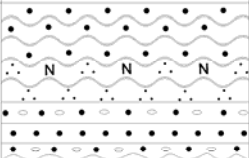
Group	Formation	Thickness	Lithological Log	Sample	Lithologic Description
Bayan Obo Group	Hujiertu	2550m		★JN2013-8	quartz sandstone, sandy slate, meta-quartz sandstone, argillaceous limestone, calcibreccia, stromatolitic limestone, siliceous limestone and interbedded slate
	Baiyinbaolage	1693m		★JN2013-6	quartzite, sandy slate and siliceous slate with interbedded meta-quartz sandstone
	Bilute	2548m		★JN2013-5	sandstone with interbedded slate, the upper part is spotted slate, sandy slate and carbonaceous slate
	Halahuogete	866m		★JN2013-3	conglomerates, sandstone, feldspathic quartz sandstone, calcareous sandstone and sandy limestone
	Jianshan	726m		★JN2013-2	quartz sandstone, slate, dolomite and limestone
	Dulahala	1010m		★JN2013-1	conglomerates, feldspathic quartz sandstones, quartzite, sandy slate and metasandstone
Basement					Archean–Paleoproterozoic gneiss

Fig. 2. The stratigraphic frame of the Bayan Obo Group (after Zhong et al., 2015; Liu C H et al., 2017).

Town (Position: N41°48'25", E113°13'55"). The outcrop is metamorphic fine-grained quartz sandstone. Its main mineral is quartz with a particle size from 0.5–1 mm and the content is 95%. The cement is mainly sericite with content of about 5% (Fig. 5e).

Sample JN2013–8 was collected from Hujiertu

Formation and its location was about 1.5 km south of Xijingzi Town (Position: N 41°47'03", E 113°12'59"). The sample is metamorphic fine-grained quartz sandstone, the size of quartz in the sample is 0.05–0.1 mm with a content of about 85%, the rest 15% is sericite recrystallized from muddy (Fig. 5f).

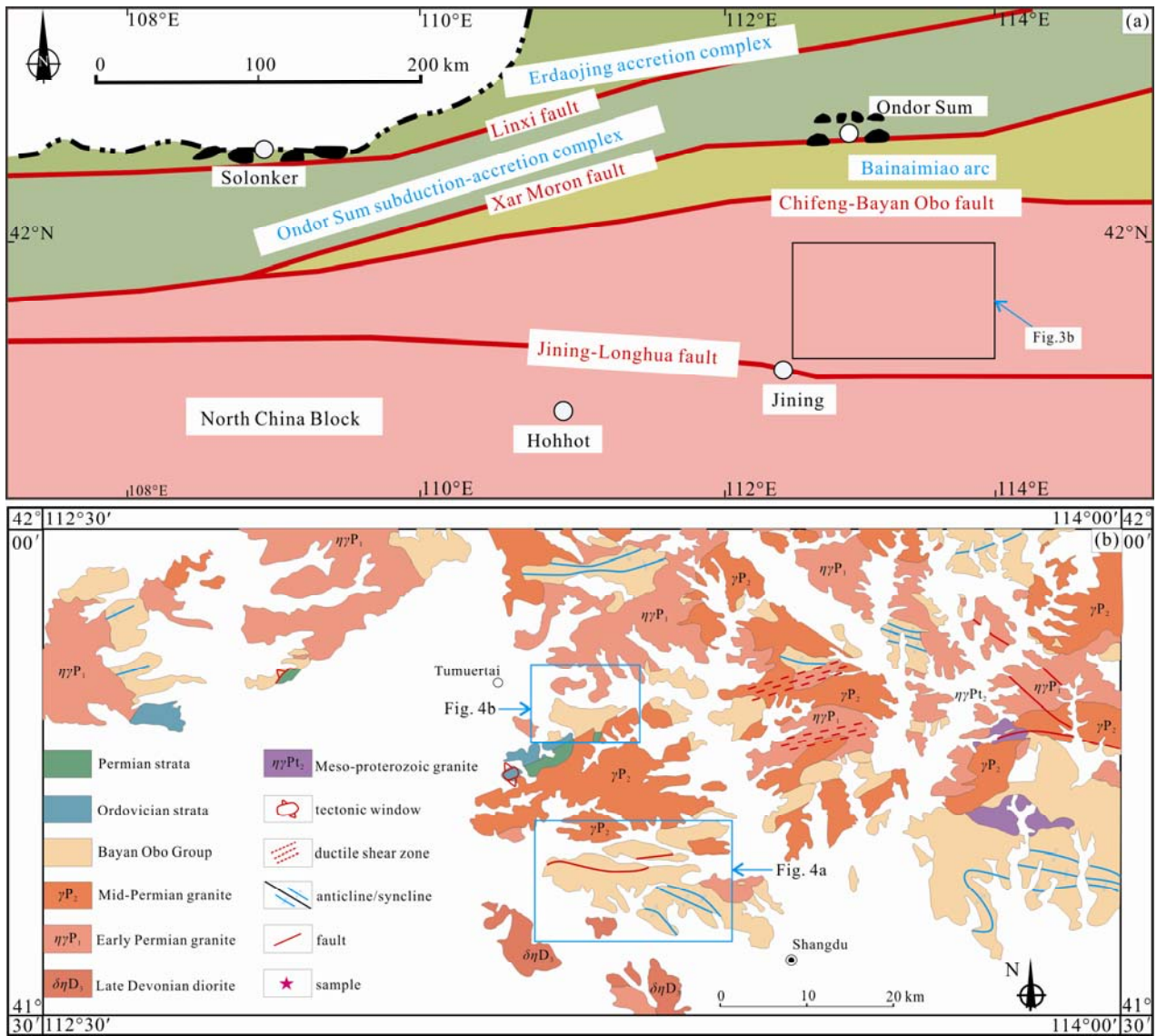


Fig. 3. (a) Tectonic division of north margin of North China Craton (after Xiao et al., 2003); (b) geologic sketch map of Shangdu area (after Wang W Q et al., 2013).

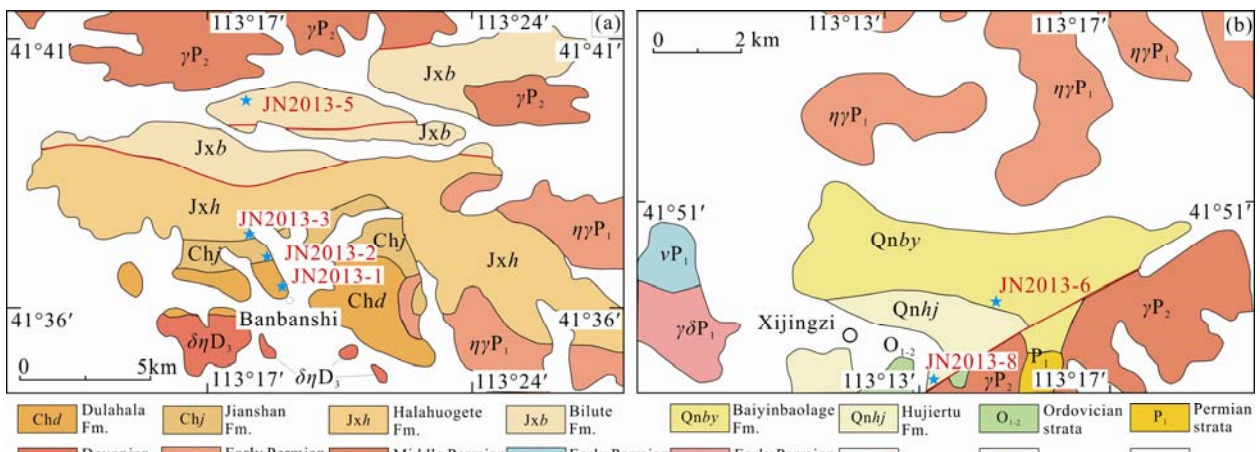


Fig. 4. (a) Geologic map of Banbanshi area and locations of samples; (b) geologic map of Xijingzi area and locations of samples (after Wang W Q et al., 2013).

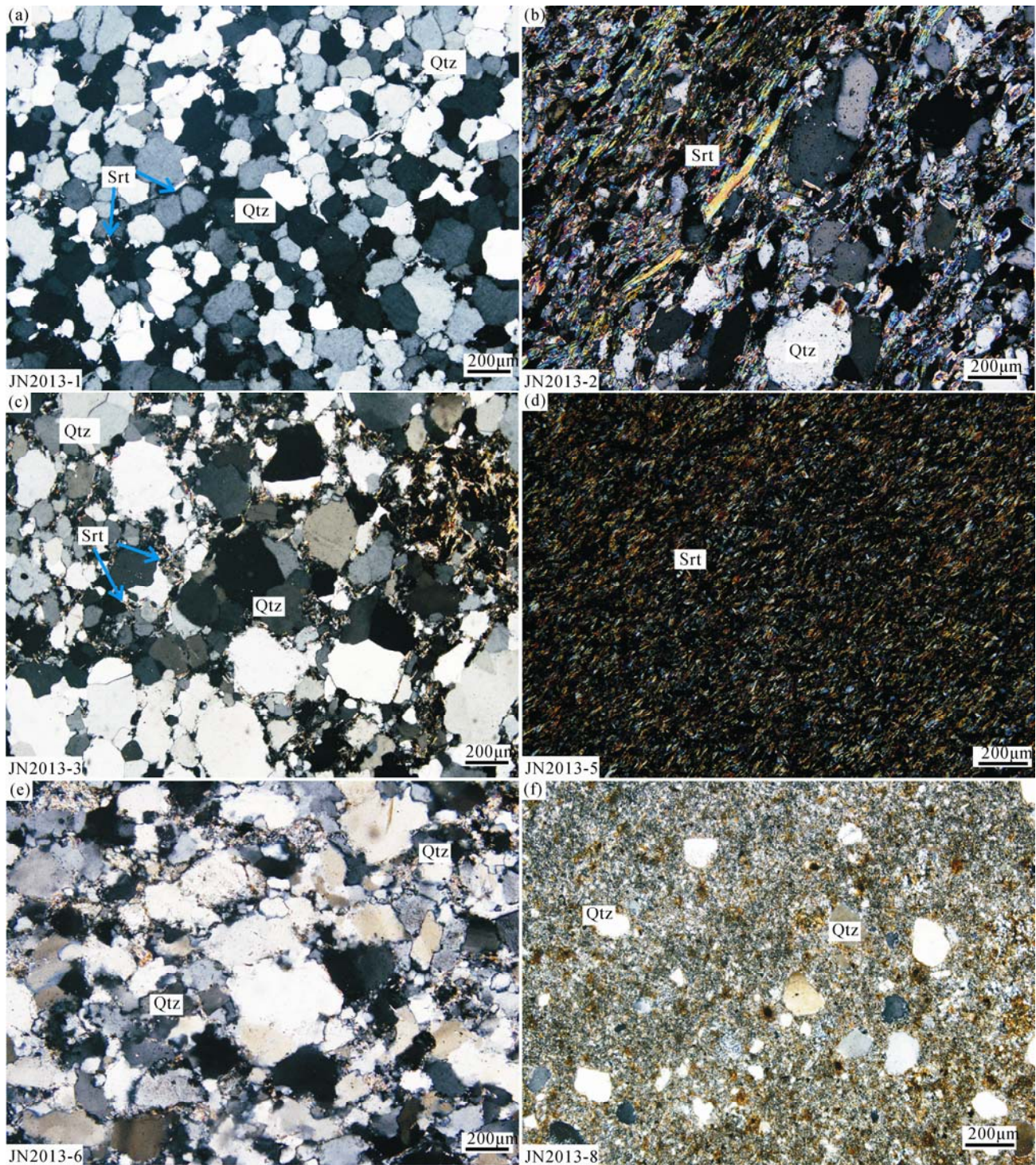


Fig. 5. Microscopic pictures of each sample from Bayao Obo Group.

(a) fine grained matrix-quartz sandstone from Dulahala, composed by 95% quartz (Qtz) and 5% Sericite(Srt); (b) sericite phyllite from Jianshan, cement is Sericite; (c) pebble-bearing matrix-coarse grained quartz sandstone from Halahuogete; (d) carbonaceous sericite phyllite, composed by flake sericite (95%); (e) metamorphic fine-grained quartz sandstone from Baiyinbaolage, made up by 95% quartz; (f) metamorphic fine-grained quartz sandstone from Hujiertu, contains few quartz pebbles.

3.2 Methods

The separation process of zircons was completed in the Keda Rock Mineral Separation Company in Langfang City, Hebei Province. The samples were crushed to the appropriate particle size and then separated using

gravitational and magnetic separating methods. The separated zircons were examined by stereo binocular. Finally, selected zircons were put on an epoxy resin disk and polished to expose their surfaces. After photographing in both reflected and transmitted light, CL

(cathodoluminescence) imaging was taken by a JSM6510 SEM attached with a Gatan CL detector.

LA-ICP-MS U-Pb zircons dating was carried out at the Key Laboratory of Mineral Resources Evaluation in Northeast Asia, Ministry of Natural Resources, Jilin University, Changchun, China. Helium was used as carrier gas to provide efficient aerosol transport to the ICP and minimize aerosol deposition around the ablation site and within the transport tube (Eggins et al., 1998; Jackson et al., 2004). Argon was used as the make-up gas and was mixed with the carrier gas via a T-connector before entering the ICP. The analysis spots were 32 μm in diameter. U, Th and Pb concentrations were calibrated using ^{29}Si as an internal standard. The standard zircon 91500 was used as an external standard to normalize isotopic fractionation during analysis. Analytical procedures used follow those described by Yuan et al., (2004). Raw data were processed using the ICPMSDataCal program (Liu et al., 2009; Liu et al., 2010). Uncertainties of individual analyses were reported with 1σ error; weighted mean ages were calculated at 1σ confidence level. Common lead correction was made following the method of Anderson (2002). The data were processed using the ISOPLOT (Version 3.0) program (Ludwig, 2003).

4 Results

We show the ages of detrital zircons from six formations of Bayan Obo Group. The reliable data with concordance between 90% and 110% were selected for further analysis. For most of ages were older than 1000 Ma, we used the $^{207}\text{Pb}/^{206}\text{Pb}$ age to make the binned frequency histograms and calculate weighted average age.

Sample JN2013-1 was collected from the Dulahala Formation. Its zircons are columnar or granular, with a particle size of 100–150 μm . They are well rounded showing the characteristics of transportation. Th/U ratio varies from 0.14 to 2.34, implying these zircons are magmatic. However, on the CL images, most of the zircons show weak oscillatory zones indicating the magmatic zircons have undergone slight recrystallization (Fig. 6). 25 reliable data points are obtained from 60 zircons (Table 1). These ages fall into a range from 1737 Ma to 2472 Ma with a major age peak at 1860 Ma and a minor peak at 2440 Ma. At the same time, a group of 6 zircons yields the youngest weighted mean $^{207}\text{Pb}/^{206}\text{Pb}$ age at 1783 ± 28 Ma ($n=6$, MSWD=1.10) (Fig. 7a), representing the maximum depositional age of the Dulahala Formation.

Sample JN2013-2 was collected from the Jianshan Formation. The zircons separated from this sample is columnar or granular with

Table 1 LA-ICP-MS zircon U-Pb data of Dulahala Formation (JN2013-1)

Sample Number	Content (ppm)		Th/U	Yb/SmN	Isotopic Elements Ratio				Age (Ma)				Concordance 100%						
	Th	U			$^{207}\text{Pb}/^{206}\text{Pb}$	1σ	$^{207}\text{Pb}/^{235}\text{U}$	1σ	$^{206}\text{Pb}/^{238}\text{U}$	1σ	$^{206}\text{Pb}/^{238}\text{U}$	1σ		$^{207}\text{Pb}/^{235}\text{U}$	1σ				
JN2013-1-02	1655.4	708.6	2.34	32.67	0.1157	0.0032	5.5675	0.1488	0.3518	0.0050	0.0617	0.0044	1891	48	1911	23	1943	24	103
JN2013-1-04	3522.2	4196.1	0.84	55.51	0.1088	0.0025	5.2549	0.1337	0.3497	0.0041	0.0559	0.0065	1789	42	1862	22	1933	19	108
JN2013-1-05	1446.9	1347.4	1.07	72.87	0.1076	0.0029	4.7456	0.1432	0.3204	0.0048	0.0504	0.0072	1759	50	1775	25	1792	23	102
JN2013-1-06	1176.8	706.6	1.67	37.93	0.1615	0.0045	10.3800	0.3108	0.4686	0.0069	0.0633	0.0108	2472	47	2469	28	2477	30	100
JN2013-1-07	707.3	992.9	0.71	64.62	0.1148	0.0034	5.1835	0.1643	0.3300	0.0055	0.0485	0.0099	1877	48	1850	27	1838	27	98
JN2013-1-08	922.7	842.7	1.10	33.77	0.1120	0.0040	5.3028	0.2026	0.3455	0.0060	0.0446	0.0107	1832	65	1869	33	1913	29	104
JN2013-1-10	1018.9	4512.6	0.23	56.82	0.1145	0.0036	5.5567	0.1980	0.3531	0.0057	0.0413	0.0134	1873	56	1909	31	1949	27	104
JN2013-1-33	125.7	73.5	1.71	67.95	0.1144	0.0041	5.2289	0.1817	0.3349	0.0071	0.1198	0.0037	1872	70	1857	30	1862	34	99
JN2013-1-34	148.7	165.3	0.90	24.11	0.1140	0.0026	5.4910	0.1311	0.3466	0.0044	0.1476	0.0037	1865	42	1899	21	1919	21	103
JN2013-1-35	83.0	593.6	0.14	22.79	0.1101	0.0021	4.8587	0.1029	0.3172	0.0043	0.1672	0.0046	1811	34	1795	18	1776	21	98
JN2013-1-36	109.7	148.1	0.74	52.42	0.1565	0.0031	10.0995	0.2098	0.4646	0.0054	0.2575	0.0047	2420	35	2444	19	2460	24	102
JN2013-1-40	44.0	85.8	0.51	19.73	0.1119	0.0028	5.0953	0.1201	0.3307	0.0045	0.2967	0.0072	1831	46	1835	20	1842	22	101
JN2013-1-41	394.5	349.2	1.13	44.55	0.1063	0.0015	4.9954	0.0696	0.3392	0.0032	0.3435	0.0041	1737	26	1819	12	1883	15	108
JN2013-1-43	131.0	189.7	0.69	15.19	0.1108	0.0019	5.1880	0.0944	0.3378	0.0037	0.3275	0.0046	1813	30	1851	15	1876	18	103
JN2013-1-44	86.3	131.6	0.66	16.60	0.1154	0.0028	5.3061	0.1413	0.3330	0.0058	0.2401	0.0060	1887	43	1870	23	1853	28	98
JN2013-1-45	73.6	154.8	0.48	46.14	0.1122	0.0026	4.9405	0.1069	0.3202	0.0049	0.2652	0.0066	1836	41	1809	18	1791	24	98
JN2013-1-46	199.8	276.6	0.72	39.91	0.1124	0.0024	5.0200	0.1102	0.3254	0.0061	0.2357	0.0042	1839	40	1823	19	1816	30	99
JN2013-1-48	360.1	600.9	0.60	68.69	0.1156	0.0020	5.3151	0.1259	0.3345	0.0078	0.1953	0.0049	1889	31	1871	20	1860	38	99
JN2013-1-49	147.2	427.8	0.34	84.22	0.1138	0.0023	5.0389	0.1205	0.3210	0.0060	0.1578	0.0047	1862	37	1826	20	1795	29	96
JN2013-1-50	70.0	121.4	0.58	33.59	0.1115	0.0029	5.0957	0.1513	0.3314	0.0064	0.1375	0.0055	1824	48	1835	25	1845	31	101
JN2013-1-51	245.9	151.5	1.62	32.57	0.1165	0.0042	5.5513	0.2213	0.3454	0.0085	0.0578	0.0054	1906	64	1909	34	1912	41	100
JN2013-1-52	193.8	666.2	0.29	88.28	0.1155	0.0028	5.0096	0.1605	0.3202	0.0104	0.0573	0.0049	1887	45	1821	27	1791	51	95
JN2013-1-54	272.4	815.0	0.33	33.04	0.1134	0.0024	5.0289	0.1533	0.3260	0.0103	0.0617	0.0042	1854	38	1824	26	1819	50	98
JN2013-1-55	529.6	498.4	1.06	42.34	0.1108	0.0027	4.9818	0.1569	0.3293	0.0094	0.0617	0.0037	1813	45	1816	27	1835	46	101
JN2013-1-58	1792.9	2051.5	0.87	41.67	0.1128	0.0018	4.9815	0.1339	0.3230	0.0096	0.0641	0.0024	1856	30	1816	23	1804	47	97

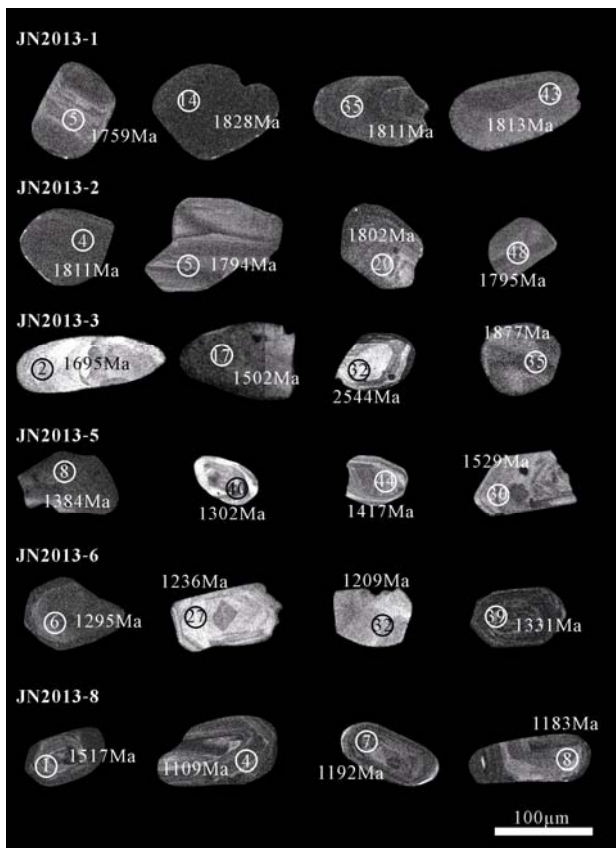


Fig. 6. Representative selection of cathodoluminescence (CL) zircon images with positions of spots, their numbers and ^{207}Pb – ^{206}Pb ages.

diameter ranging from 100–130 μm . Th/U ratio of these zircons is between 0.16 and 6.96 and some zircons have oscillatory zones, implying they are magmatic. But the zircons with weak growth zones or without may be magmatic and underwent metamorphism or recrystallization (Fig. 6). The 20 reliable ages data distribute between 1794 Ma and 2473 Ma (Table 2), the minimum weighted mean age is 1807 ± 44 Ma ($n=5$, $\text{MSWD}=0.109$) (Fig. 7b), representing the maximum depositional age of the Jianshan Formation.

The zircons of Sample JN2013–3 collected from Halahuogete Formation are columnar or granular and their length to width ratio is 1:1–2:1, showing well-grinded characteristics. Most of the zircons show oscillatory zones implying magmatic origin, and a few of them are metamorphic or recrystallized zircons (Fig. 6). 32 reliable ages were acquired from 60 zircons (Table 3). The ^{207}Pb – ^{206}Pb ages vary from 1861 Ma to 2613 Ma, and the youngest weighted mean age is 1878 ± 28 Ma ($n=4$, $\text{MSWD}=0.13$) (Fig. 7c) which is the maximum sedimentary age of Halahuogete Formation.

Sample JN2013–5 was collected from the Bilute Formation. The zircons are ellipsoidal or granular with size between 80 and 120 μm . The CL images show that both magmatic and recrystallized zircons are present (Fig. 6). The Th/U ratio is between 0.29 and 1.81. A total of 26

Table 2 LA–ICP–MS zircon U–Pb data of Jianshan Formation (JN2013–2)

Sample Number	Content (ppm)		Th/U	Yb/Sm/N	Isotopic Elements Ratio			Age (Ma)			Concordance								
	Th	U			$^{207}\text{Pb}/^{235}\text{U}$	$^{206}\text{Pb}/^{238}\text{U}$	$^{207}\text{Pb}/^{206}\text{Pb}$	$^{207}\text{Pb}/^{235}\text{U}$	$^{206}\text{Pb}/^{238}\text{U}$	σ									
JN2013-2-01	5083.8	3785.3	1.34	13.5	0.0037	5.4589	0.1749	0.3399	0.0071	0.0531	0.0213	1869	59	1894	28	1886	34	101	
JN2013-2-02	948.6	6013.4	0.16	12.5	0.0032	5.5730	0.1548	0.3490	0.0061	0.0509	0.0200	1850	52	1912	24	1930	29	104	
JN2013-2-04	22317.4	9597.0	2.33	7.8	0.1107	0.0025	5.2438	0.1255	0.3335	0.0054	0.0262	1811	42	1860	20	1855	26	102	
JN2013-2-05	16361.2	5790.5	2.83	6.4	0.1096	0.0024	5.2299	0.1169	0.3353	0.0047	0.0256	1794	41	1858	19	1864	23	104	
JN2013-2-08	4341.8	1831.1	2.37	35.9	0.1423	0.0027	9.0593	0.1989	0.4462	0.0075	0.0386	0.0107	2255	33	2344	20	2378	34	105
JN2013-2-11	4570.4	983.5	4.65	25.9	0.1494	0.0031	9.5803	0.2313	0.4474	0.0079	0.0239	2339	35	2395	22	2384	35	102	
JN2013-2-13	12490.3	4728.6	2.64	11.9	0.1125	0.0018	5.2412	0.1083	0.3279	0.0060	0.0091	1840	60	1859	18	1828	29	99	
JN2013-2-19	8240.8	2829.7	2.91	10.3	0.1151	0.0028	5.6715	0.1429	0.3516	0.0049	0.0022	1881	44	1927	22	1942	32	103	
JN2013-2-20	11546.9	1658.9	6.96	8.5	0.1102	0.0034	5.2094	0.1776	0.3379	0.0066	0.0355	1802	56	1854	29	1877	23	104	
JN2013-2-24	2732.9	532.9	5.13	27.7	0.1129	0.0087	5.2064	0.3925	0.3349	0.0046	0.0046	1846	140	1854	64	1862	70	101	
JN2013-2-25	2895.6	1004.7	2.88	36.1	0.1237	0.0042	6.5861	0.2098	0.3848	0.0071	0.0585	2010	60	2057	28	2098	33	104	
JN2013-2-26	6783.0	1502.7	4.51	41.8	0.1230	0.0049	6.7340	0.2767	0.3921	0.0074	0.0597	2067	71	2077	36	2133	34	103	
JN2013-2-31	13510.3	3793.0	3.56	60.7	0.1508	0.0017	9.7495	0.1414	0.4606	0.0052	0.0029	2355	19	2411	13	2442	23	104	
JN2013-2-40	3777.1	1779.8	2.12	31.8	0.1327	0.0014	8.0419	0.1288	0.4251	0.0067	0.0306	2200	20	2236	14	2283	30	104	
JN2013-2-45	170.9	139.0	1.23	57.0	0.1489	0.0023	9.4966	0.1839	0.4515	0.0074	0.0322	2344	26	2387	18	2402	33	102	
JN2013-2-48	155.9	148.8	1.05	25.3	0.1097	0.0041	4.8088	0.1818	0.3150	0.0066	0.0181	1795	69	1786	32	1765	33	98	
JN2013-2-50	551.0	268.7	2.05	23.1	0.1534	0.0024	9.7102	0.1560	0.4556	0.0063	0.0330	2384	26	2408	15	2420	28	101	
JN2013-2-51	162.4	97.7	1.66	37.9	0.1616	0.0030	10.2224	0.3097	0.4592	0.0115	0.0374	2473	33	2455	28	2436	51	99	
JN2013-2-58	99.7	191.9	0.52	36.1	0.1172	0.0026	5.8329	0.1550	0.3641	0.0058	0.0038	1913	40	1951	23	2001	27	105	
JN2013-2-60	76.7	188.4	0.41	77.4	0.1261	0.0029	6.8782	0.2026	0.3982	0.0061	0.0597	2056	39	2096	26	2161	28	105	

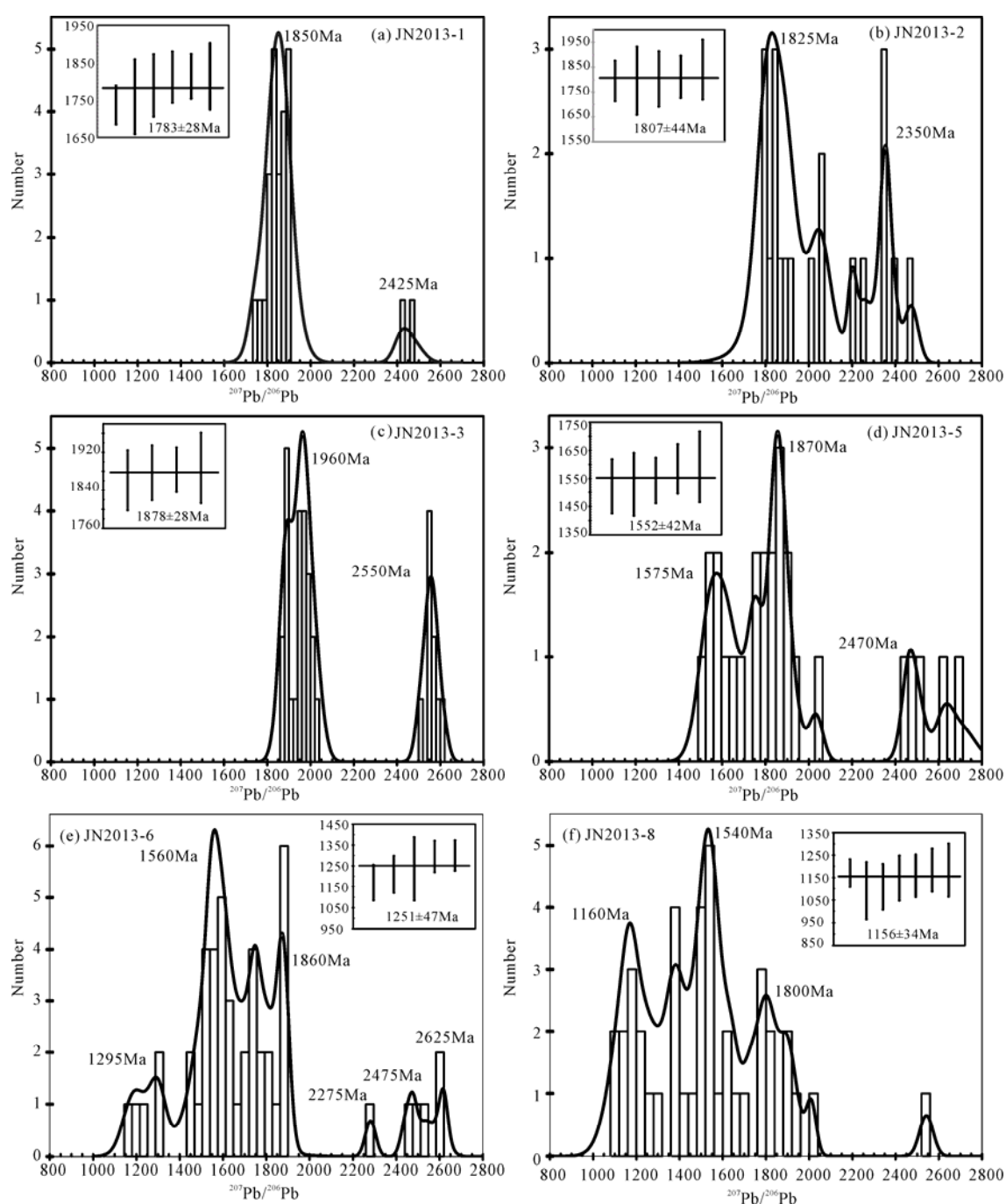


Fig. 7. Weighted average age and binned frequency histograms of zircon ages for each sample from the Bayan Obo Group.

data were obtained from 60 zircons (Table 4). The zircon ages range from 1522 Ma to 2706 Ma and the youngest group of five zircons yields the weighted mean age at 1552 ± 42 Ma ($n=5$, $MSWD=0.38$) (Fig. 7d), indicating Bilute Formation deposited after that.

Sample JN2013-6 was collected from Baiyinbaolage Formation. Zircons are ellipsoidal or granular, with size of 80–100 μm and length to width ratio at 1:1–1:2. According to the characteristics of CL images, the zircons can be divided into magmatic, recrystallized and

metamorphic zircons (Fig. 6). 48 reliable ages were obtained from 60 zircons, ranging between 1170 Ma and 2618 Ma (Table 5). The ages of zircons mainly cluster in five ranges, which are 1.17–1.30 Ga, 1.44–1.60 Ga, 1.61–1.79 Ga and 1.81–1.88 Ga respectively. Most of zircons with ages younger than 1700 Ma are magmatic zircons with recrystallized characteristics and their Th/U ratio is between 0.21 and 1.85. A group of youngest zircons give the weighted mean age at 1251 ± 74 Ma ($n=5$, $MSWD=1.9$) (Fig. 7e), which represents the lower boundary of the

Baiyinbaolage Formation.

Sample JN2013–8 was collected from Hujertu Formation. The zircons from this formation is granular or round, with a size of 80–100 μm . A total of 41 age data are obtained from 60 zircons (Table 6). The ages range between 1092 Ma and 2542 Ma with the Th/U ratio between 0.30 and 4.19. Combined with the characteristics of CL images, magmatic zircons are dominant in this sample, while a small number of metamorphic zircons also exist (Fig. 6). Ages of zircons mainly concentrate in the following ranges: 1.02–1.29 Ga, 1.34–1.49 Ga, 1.51–1.57 Ga, 1.62–1.79 Ga and 1.81–2.54 Ga. The youngest weighted mean age is 1156 ± 34 Ma ($n=7$, MSWD=0.44) (Fig. 7f), which indicates Hujertu Formation deposited after that.

5 Discussions

5.1 Depositional age of Bayan Obo Group

Actually, it is controversial with the sedimentary age of the Bayan Obo Group. The disputes mainly focused on whether it deposited in the early Paleozoic (Sun, 1992; Tan et al., 2000) or the Meso- to Neoproterozoic. However, the idea of regarding it as early Paleozoic strata has not been supported by convincing fossils evidences. In recent years, great progresses have been made in the chronological study of Jixian standard section in the Yanliao rift zone and the depositional age of this strata has been revised. The sedimentary age of the Changcheng System was 1650 Ma–1600 Ma, that of Jixian System was 1600–1400 Ma, and 1400–1000 Ma was Awaiting System, the age of Qingbaikou was younger than 1000 Ma (Li et al., 2013). This revised age of Jixian standard section provides a reference for the comparison of strata in the northern margin of NCC. Based on our newly obtained age data of detrital zircons and previous research results, the depositional age of Bayan Obo Group is discussed in this paper.

The youngest weighted mean $^{207}\text{Pb}/^{206}\text{Pb}$ ages obtained from Dulahala Formation and Jianshan Formation are 1783 ± 28 Ma ($n=6$, MSWD=1.10) and 1807 ± 44 Ma ($n=5$, MSWD=0.109) respectively. The minimum ages of detrital zircons from Dulahala Formation given by previous studies include 1827 Ma (Ma M Z et al., 2014), 1822 ± 9 Ma ($n=3$, MSWD = 0.72) (Zhong et al., 2015), 1809 ± 9 Ma ($n=3$, MSWD=0.72) (Zhou et al., 2018). Meanwhile, the youngest detrital zircon ages from Jianshan Formation published by predecessors include 1716 Ma, 1810 Ma (Zhou et al., 2018), 1847 Ma (Zhong et al., 2015). Combined with the ~1743 Ma basic volcanic interlayer at the bottom of the Zha'ertai Group (Li et al., 2007), the ~1670 Ma gabbro intruding into Dulahala Formation (Zhou et al., 2016) and the whole rock $^{207}\text{Pb}/^{206}\text{Pb}$

Table 3 LA-ICP-MS zircon U–Pb data of Halahege Formation (JN2013-3)

Sample Number	Content (ppm)		Th/U	Yb/Sm _N	Isotopic Elements Ratio				Age (Ma)				Concordance 100%						
	Th	U			$^{207}\text{Pb}/^{235}\text{U}$	$^{206}\text{Pb}/^{238}\text{U}$	$^{206}\text{Pb}/^{232}\text{Th}$	$^{207}\text{Pb}/^{206}\text{Pb}$	$^{207}\text{Pb}/^{235}\text{U}$	$^{206}\text{Pb}/^{238}\text{U}$	$^{207}\text{Pb}/^{235}\text{U}$	$^{206}\text{Pb}/^{238}\text{U}$							
JN2013-3-21	167.2	466.9	0.36	18.8	0.1240	0.0021	6.2180	0.1168	0.3626	0.0038	0.0738	0.0059	2017	35	2007	16	1995	18	99
JN2013-3-22	85.0	111.7	0.76	43.2	0.1706	0.0028	11.4545	0.2056	0.4863	0.0049	0.1646	0.0103	2565	28	2561	17	2555	21	100
JN2013-3-23	116.1	180.1	0.64	46.2	0.1162	0.0024	5.3767	0.1011	0.3355	0.0037	0.1170	0.0067	1898	31	1881	16	1865	18	98
JN2013-3-24	69.0	103.5	0.67	53.4	0.1154	0.0020	5.2426	0.1092	0.3292	0.0031	0.1157	0.0063	1887	37	1860	18	1834	15	97
JN2013-3-25	78.9	88.8	0.89	53.8	0.1692	0.0028	11.2327	0.1853	0.4819	0.0047	0.1679	0.0085	2550	28	2543	15	2535	21	99
JN2013-3-27	270.2	363.4	0.74	12.8	0.1158	0.0016	5.4034	0.0772	0.3377	0.0027	0.1177	0.0055	1892	25	1885	12	1876	13	99
JN2013-3-30	115.0	211.6	0.54	62.1	0.1158	0.0017	5.4273	0.0859	0.3396	0.0039	0.1235	0.0063	1892	28	1889	14	1885	19	100
JN2013-3-31	150.6	191.7	0.79	87.3	0.1138	0.0020	5.2774	0.0871	0.3363	0.0032	0.1241	0.0071	1861	31	1865	14	1869	16	100
JN2013-3-32	77.1	51.3	1.50	31.5	0.1686	0.0035	10.9783	0.2428	0.4721	0.0059	0.1671	0.0089	2544	40	2521	21	2493	26	98
JN2013-3-33	83.0	675.2	0.12	66.9	0.1152	0.0015	5.3140	0.0706	0.3338	0.0028	0.1087	0.0055	1883	23	1871	11	1857	14	99
JN2013-3-35	121.8	167.2	0.73	24.9	0.1148	0.0018	5.2501	0.0903	0.3308	0.0032	0.1187	0.0054	1877	29	1861	15	1842	15	98
JN2013-3-36	69.9	212.7	0.33	17.2	0.1647	0.0022	10.7536	0.1466	0.4725	0.0037	0.1693	0.0076	2505	22	2502	13	2495	16	100
JN2013-3-37	112.8	345.0	0.33	42.6	0.1202	0.0017	5.7139	0.0754	0.3449	0.0030	0.1324	0.0060	1959	19	1933	11	1910	14	98
JN2013-3-38	103.9	424.3	0.24	117.9	0.1192	0.0015	5.7296	0.0841	0.3480	0.0034	0.1274	0.0059	1944	22	1936	13	1925	16	99
JN2013-3-39	81.8	128.2	0.64	35.5	0.1184	0.0020	5.6951	0.0983	0.3486	0.0035	0.1267	0.0061	1933	29	1931	15	1928	17	100
JN2013-3-40	38.1	426.5	0.09	78.0	0.1213	0.0017	6.0223	0.0918	0.3600	0.0038	0.1284	0.0067	1976	58	1979	13	1982	18	100
JN2013-3-41	129.6	325.0	0.40	87.1	0.1219	0.0019	5.8392	0.0990	0.3472	0.0032	0.1304	0.0076	1984	23	1952	15	1921	15	97
JN2013-3-42	77.0	239.5	0.32	31.4	0.1233	0.0028	6.0746	0.1521	0.3571	0.0054	0.1322	0.0077	2006	41	1987	22	1969	26	98
JN2013-3-43	263.2	119.7	2.20	21.4	0.1204	0.0022	5.7368	0.1128	0.3453	0.0032	0.1319	0.0070	1963	33	1937	17	1912	15	97
JN2013-3-45	154.9	316.6	0.49	67.7	0.1725	0.0022	11.6677	0.1576	0.4899	0.0037	0.1895	0.0105	2583	21	2578	13	2570	16	99
JN2013-3-47	79.0	128.4	0.62	4.5	0.1224	0.0021	5.9354	0.1077	0.3511	0.0031	0.1512	0.0096	1992	36	1966	16	1940	15	97
JN2013-3-48	60.0	153.6	0.39	45.4	0.1203	0.0019	5.6361	0.0906	0.3396	0.0027	0.1513	0.0103	1961	29	1922	14	1885	13	96
JN2013-3-49	51.7	134.7	0.38	55.0	0.1164	0.0027	5.3248	0.1178	0.3321	0.0036	0.1515	0.0113	1902	41	1873	19	1849	17	97
JN2013-3-50	58.3	358.8	0.16	147.1	0.1197	0.0018	5.6004	0.0866	0.3389	0.0032	0.1489	0.0119	1952	33	1916	13	1881	15	96
JN2013-3-51	130.5	235.5	0.55	44.3	0.1201	0.0021	5.6451	0.0972	0.3410	0.0035	0.1567	0.0142	1958	30	1923	15	1891	17	97

isochron age of sedimentary carbonate rock at 1649±45 Ma (Yang et al., 2012), it can be preliminarily concluded that the sedimentary age from Dulahala to Jianshan Formation at the bottom of the Bayan Obo Group was 1800–1650 Ma.

The youngest $^{207}\text{Pb}/^{206}\text{Pb}$ weighted mean age of detrital zircons obtained from Halahuogete Formation is 1878±28 Ma (n=4, MSWD=0.13). While the youngest weighted mean $^{207}\text{Pb}/^{206}\text{Pb}$ age given by detrital zircons from Bilute Formation is 1552±42 Ma (n=5, MSWD=0.38). The youngest detrital zircons ages from the above two formations are roughly equal to those from the previous studies, such as 1834–1757 Ma from Halahuogete Formation (Liu C H et al., 2017; Zhong et al., 2015) and 1561±40 Ma from Bilute Formation (Liu C H et al., 2017). It is worth noting that Halahuogete Formation exhibits characteristics of local cycling (Liu C H et al., 2017), therefore its true depositional age might be much younger than the maximum depositional age of this formation. Given the H_8 ore-bearing dolomite from Bayan Obo Group yielded Sm–Nd isotopic age at 1341±160 Ma (Yang et al., 2011) and $^{232}\text{Th}/^{208}\text{Pb}$ age at 1325±60 Ma (Campbell et al., 2014), gabbro intruded into Bilute Formation with age of 1342±9 Ma (Zhou et al., 2016), granites intruded into the middle of Bayan Obo Group with age between 1313 and 1331 Ma (Shi et al., 2012; Zhang et al., 2012), this paper believes that the depositional age of Halahuogete to Bilute Formation in the middle part of the Bayan Obo Group was between 1500 and 1350 Ma, comparable to Jixian System (1600–1400 Ma) (Li et al., 2013). This result is consistent with the previous conclusion that the middle part of Bayan Obo Group deposited between 1.56–1.35 Ga (Zhong et al., 2015; Liu C H et al., 2017).

The youngest weighted mean $^{207}\text{Pb}/^{206}\text{Pb}$ age of detrital zircons from Baiyinbaolage and Hujertu Formation is 1251±74 Ma (n=5, MSWD=1.9) and 1156±34 Ma (n=7, MSWD=0.44) respectively. The above results are consistent with the previously reported youngest weighted mean $^{207}\text{Pb}/^{206}\text{Pb}$ age at 1250 Ma for Baiyinbaolage Formation and 1116–1144 Ma for Hujertu Formation respectively (Zhou et al., 2018; Liu C H et al., 2017). According to the ~900 Ma basic dykes intruding into Neoproterozoic strata in the eastern part of North China Craton, the upper sedimentary age of Bayan Obo Group was temporarily placed at 900 Ma through regional stratigraphic comparison (Peng et al., 2011a, 2011b). Therefore, the depositional age of the Baiyinbaolage to the Hujertu Formation were between 1250 Ma and 900 Ma, which is

Table 4 LA-ICP-MS zircon U–Pb data of Bilute Formation (JN2013-5)

Sample Number	Content (ppm)		Th/U	Yb/Sm _N	$^{207}\text{Pb}/^{206}\text{Pb}$		Isotopic Elements Ratio		Age (Ma)		Concordance						
	Th	U			$^{207}\text{Pb}/^{206}\text{Pb}$	1σ	$^{207}\text{Pb}/^{235}\text{U}$	1σ	$^{206}\text{Pb}/^{232}\text{Th}$	1σ	$^{207}\text{Pb}/^{235}\text{U}$	1σ	$^{206}\text{Pb}/^{238}\text{U}$	1σ			
JN2013-5-05	144.0	495.7	0.29	51.1	0.1143	0.0022	5.1953	0.1250	0.3288	0.0056	0.0578	0.0067	1852	20	1833	27	98
JN2013-5-06	320.6	767.2	0.42	4.3	0.1157	0.0020	4.8967	0.1022	0.3056	0.0040	0.0528	0.0030	1802	18	1719	20	91
JN2013-5-09	308.9	333.9	0.92	60.3	0.1177	0.0026	5.5416	0.1279	0.3422	0.0056	0.0695	0.0050	1907	20	1897	27	99
JN2013-5-12	518.1	451.7	1.15	53.2	0.1139	0.0021	5.0379	0.0918	0.3201	0.0037	0.0726	0.0033	1826	15	1790	18	96
JN2013-5-14	1125.7	1082.6	1.04	35.4	0.1122	0.0017	5.1209	0.0842	0.3304	0.0046	0.0736	0.0054	1840	14	1840	22	100
JN2013-5-16	230.9	294.5	0.78	20.1	0.1770	0.0044	11.7396	0.3089	0.4780	0.0071	0.1099	0.0114	2584	25	2519	31	96
JN2013-5-17	428.9	1008.8	0.43	7.3	0.1246	0.0023	5.6823	0.1153	0.3287	0.0053	0.0801	0.0095	1929	18	1832	26	90
JN2013-5-18	608.4	336.7	1.81	17.7	0.1154	0.0034	5.1424	0.1359	0.3235	0.0049	0.0727	0.0096	1887	53	1807	24	96
JN2013-5-19	520.2	865.9	0.60	107.0	0.0942	0.0024	3.3091	0.0955	0.2528	0.0041	0.0612	0.0090	1522	48	1453	21	95
JN2013-5-22	1171.9	901.7	1.30	74.9	0.1027	0.0033	3.9602	0.1416	0.2771	0.0052	0.0626	0.0110	1626	29	1577	26	94
JN2013-5-29	227.9	277.3	0.82	96.3	0.0979	0.0025	3.8527	0.1045	0.2844	0.0039	0.0547	0.0060	1604	22	1614	20	102
JN2013-5-30	156.2	173.4	0.90	69.6	0.0951	0.0028	3.5536	0.1086	0.2704	0.0040	0.0562	0.0062	1529	56	1539	24	101
JN2013-5-33	197.2	155.4	1.27	36.4	0.1103	0.0030	4.3999	0.1244	0.2888	0.0039	0.0627	0.0063	1712	23	1635	20	91
JN2013-5-34	92.2	95.1	0.97	93.1	0.1022	0.0032	3.9074	0.1276	0.2766	0.0041	0.0558	0.0052	1615	26	1574	21	95
JN2013-5-36	152.4	449.8	0.34	50.6	0.1134	0.0020	5.2156	0.1099	0.3316	0.0044	0.0696	0.0053	1855	18	1846	21	100
JN2013-5-37	187.4	204.4	0.92	122.8	0.1603	0.0029	9.9437	0.2080	0.4481	0.0058	0.0880	0.0060	2430	19	2387	26	97
JN2013-5-38	62.0	123.3	0.50	68.1	0.1859	0.0072	12.6292	0.4964	0.928	0.0109	0.1183	0.0087	2706	65	2583	47	95
JN2013-5-41	74.3	91.3	0.81	54.5	0.1102	0.0033	4.7206	0.1525	0.3102	0.0046	0.0658	0.0038	1803	55	1742	23	97
JN2013-5-42	567.9	475.1	1.20	40.9	0.0957	0.0020	3.5236	0.0825	0.2666	0.0036	0.0515	0.0028	1533	19	1523	18	99
JN2013-5-46	91.9	183.6	0.50	144.8	0.1653	0.0034	10.8502	0.2726	0.4749	0.0071	0.0923	0.0071	2510	35	2505	31	100
JN2013-5-49	382.0	767.9	0.50	24.6	0.1073	0.0021	4.4795	0.1001	0.3021	0.0037	0.0575	0.0061	1727	19	1702	18	97
JN2013-5-52	126.9	131.4	0.97	99.7	0.0983	0.0033	3.5436	0.1175	0.2632	0.0041	0.0532	0.0068	1592	63	1537	26	95
JN2013-5-53	137.2	306.5	0.45	67.7	0.0995	0.0022	4.0590	0.1028	0.2950	0.0038	0.0579	0.0067	1617	42	1667	19	103
JN2013-5-56	129.8	189.9	0.68	76.0	0.1607	0.0028	10.4548	0.2183	0.4703	0.0054	0.0972	0.0080	2476	19	2485	24	101
JN2013-5-59	148.7	199.4	0.75	73.2	0.1068	0.0020	4.5660	0.0886	0.3101	0.0033	0.0679	0.0034	1743	16	1741	16	100

Table 5 LA–ICP–MS zircon U–Pb data of Baiyibaolage Formation (JN2013–6)

Sample Number	Content (ppm)		Th/U	Yb/Sm _N	Isotopic Elements Ratio				Age (Ma)				Concordance				
	Th	U			²⁰⁷ Pb/ ²³⁵ U	σ	²⁰⁷ Pb/ ²⁰⁶ Pb	σ	²⁰⁶ Pb/ ²³² Th	σ	²⁰⁷ Pb/ ²⁰⁶ Pb	σ	²⁰⁷ Pb/ ²³⁵ U	σ	100%	σ	
JN2013-6-02	78.5	101.4	0.77	102.7	0.983	0.0027	3.7728	0.1060	0.2784	0.0030	0.0959	52	1587	23	1583	15	99
JN2013-6-03	86.5	157.2	0.55	87.9	0.1445	0.0020	8.4648	0.1260	0.4244	0.0035	0.1321	24	2282	14	2280	16	100
JN2013-6-04	393.5	310.3	1.27	80.2	0.0977	0.0014	3.7132	0.0545	0.2750	0.0021	0.0866	0.0042	1581	12	1566	10	99
JN2013-6-05	83.5	146.5	0.57	37.8	0.1148	0.0018	5.3024	0.0873	0.3347	0.0034	0.1005	0.0046	1877	28	1869	14	99
JN2013-6-06	138.4	183.4	0.75	116.1	0.0841	0.0016	2.5242	0.0532	0.2172	0.0024	0.0651	0.0028	1295	38	1279	15	98
JN2013-6-07	76.0	75.3	1.01	112.4	0.0908	0.0027	3.0589	0.0925	0.2444	0.0030	0.0718	0.0030	1443	57	1422	23	98
JN2013-6-08	81.4	169.0	0.48	18.4	0.1080	0.0021	4.6719	0.3130	0.0842	0.0032	0.0842	0.0033	1769	40	1762	17	99
JN2013-6-09	405.8	348.5	1.16	90.0	0.0986	0.0015	3.7896	0.0547	0.2791	0.0028	0.0736	0.0027	1598	30	1591	12	99
JN2013-6-10	74.1	176.8	0.42	92.7	0.1097	0.0019	4.9013	0.0908	0.3230	0.0033	0.0807	0.0033	1794	31	1802	16	101
JN2013-6-11	208.4	222.4	0.94	30.0	0.1107	0.0020	4.9139	0.0897	0.3212	0.0032	0.0704	0.0032	1811	27	1805	15	99
JN2013-6-12	169.5	328.6	0.52	85.8	0.1059	0.0018	4.4417	0.0756	0.3034	0.0026	0.0881	0.0041	1731	31	1720	14	99
JN2013-6-14	58.4	75.5	0.77	108.8	0.0992	0.0024	3.8113	0.1024	0.2783	0.0036	0.0908	0.0053	1609	46	1595	22	98
JN2013-6-15	116.5	209.2	0.56	21.6	0.1140	0.0017	5.3028	0.0841	0.3364	0.0027	0.1127	0.0072	1865	27	1869	14	100
JN2013-6-16	325.3	374.9	0.87	22.0	0.0927	0.0014	3.2656	0.0490	0.2550	0.0021	0.0965	0.0067	1481	28	1473	12	99
JN2013-6-18	127.7	178.3	0.72	88.4	0.0974	0.0018	3.7035	0.0651	0.2758	0.0023	0.1109	0.0088	1576	34	1572	14	100
JN2013-6-19	498.5	471.3	1.06	29.2	0.1014	0.0022	3.8693	0.0982	0.2754	0.0029	0.0877	0.0075	1650	45	1607	20	95
JN2013-6-20	220.3	240.2	0.92	92.0	0.1002	0.0017	3.8820	0.0692	0.2802	0.0023	0.1239	0.0108	1629	33	1610	14	98
JN2013-6-21	115.2	62.2	1.85	31.9	0.1670	0.0032	11.4053	0.2194	0.4947	0.0049	0.2212	0.0208	2528	33	2557	18	102
JN2013-6-22	76.7	108.5	0.71	132.4	0.0950	0.0023	3.4351	0.0765	0.2631	0.0025	0.1204	0.0108	1528	45	1512	18	99
JN2013-6-24	300.4	438.1	0.69	25.9	0.1591	0.0022	9.9490	0.1339	0.4527	0.0036	0.1216	0.0096	2446	24	2430	12	98
JN2013-6-26	94.6	152.5	0.62	77.4	0.1074	0.0018	4.6615	0.0831	0.3146	0.0031	0.1276	0.0086	1755	31	1760	15	100
JN2013-6-27	59.7	42.1	1.42	62.9	0.0816	0.0032	2.3796	0.0866	0.2145	0.0028	0.0857	0.0053	1236	76	1236	26	101
JN2013-6-28	112.2	132.7	0.85	76.9	0.0954	0.0017	3.4738	0.0634	0.2647	0.0028	0.1034	0.0056	1536	34	1521	14	99
JN2013-6-29	67.6	107.6	0.63	47.0	0.1146	0.0020	5.2609	0.1003	0.3322	0.0031	0.1322	0.0064	1876	31	1863	16	99
JN2013-6-31	70.8	103.0	0.69	117.3	0.0955	0.0018	3.7297	0.0681	0.2843	0.0031	0.0849	0.0012	1539	35	1578	15	105
JN2013-6-32	116.9	133.8	0.87	47.1	0.0804	0.0018	2.1778	0.0506	0.1967	0.0021	0.0516	0.0007	1209	44	1174	16	96
JN2013-6-33	174.0	159.6	1.09	53.0	0.1037	0.0015	4.2396	0.0716	0.2964	0.0034	0.0775	0.0033	1692	26	1682	14	99
JN2013-6-34	96.0	147.7	0.65	115.4	0.0954	0.0016	3.6362	0.0557	0.2775	0.0025	0.0794	0.0010	1536	30	1557	12	103
JN2013-6-35	116.0	119.4	0.97	46.6	0.1068	0.0019	4.6010	0.0878	0.3127	0.0029	0.0854	0.0010	1746	28	1754	14	100
JN2013-6-38	103.0	123.5	0.83	81.0	0.0916	0.0021	3.1683	0.0716	0.2524	0.0028	0.0673	0.0008	1461	44	1449	17	99
JN2013-6-39	172.7	251.3	0.69	90.9	0.0839	0.0016	2.7110	0.0506	0.2349	0.0019	0.0615	0.0007	1300	37	1331	14	105
JN2013-6-40	135.0	183.6	0.74	86.6	0.0789	0.0017	2.2116	0.0518	0.2032	0.0018	0.0515	0.0007	1170	43	1185	16	102
JN2013-6-41	173.0	255.8	0.68	84.5	0.0961	0.0014	3.5977	0.0577	0.2725	0.0027	0.0631	0.0007	1550	26	1549	13	100
JN2013-6-42	69.8	205.1	0.34	58.8	0.1152	0.0015	5.3186	0.0836	0.3353	0.0032	0.0689	0.0016	1883	24	1872	13	99
JN2013-6-43	179.5	268.5	0.67	76.3	0.1000	0.0012	3.8562	0.0558	0.2801	0.0028	0.0651	0.0014	1633	172	1605	12	97
JN2013-6-44	151.1	323.6	0.47	66.6	0.1069	0.0014	4.4683	0.0700	0.3034	0.0031	0.0788	0.0024	1747	23	1725	13	98
JN2013-6-45	68.6	201.4	0.34	117.2	0.1763	0.0020	12.0861	0.1765	0.4987	0.0067	0.1166	0.0037	2618	19	2611	14	100
JN2013-6-47	162.9	119.6	1.36	112.9	0.1611	0.0019	10.2311	0.1325	0.4605	0.0048	0.1210	0.0047	2478	19	2456	12	99
JN2013-6-48	58.1	99.3	0.58	112.7	0.0979	0.0021	3.6621	0.0776	0.2717	0.0032	0.0818	0.0037	1584	45	1563	17	98
JN2013-6-49	51.4	88.2	0.58	37.1	0.1123	0.0022	5.0259	0.0996	0.3253	0.0040	0.0994	0.0049	1836	36	1824	17	99
JN2013-6-50	328.2	467.5	0.70	126.4	0.0964	0.0013	3.6015	0.0482	0.2719	0.0029	0.0850	0.0043	1547	25	1550	11	100
JN2013-6-51	70.3	92.0	0.76	112.6	0.0970	0.0022	3.6861	0.0869	0.2739	0.0038	0.0891	0.0052	1576	43	1568	19	99
JN2013-6-54	62.2	162.0	0.38	69.2	0.1148	0.0020	5.2645	0.0934	0.3310	0.0035	0.1095	0.0054	1877	26	1863	15	98
JN2013-6-55	64.6	54.0	1.20	14.9	0.1085	0.0033	4.5977	0.1430	0.3066	0.0042	0.1020	0.0048	1776	57	1749	26	97
JN2013-6-57	82.1	113.7	0.72	43.4	0.1746	0.0039	11.7285	0.2778	0.4840	0.0054	0.1511	0.0072	2602	37	2583	22	98
JN2013-6-58	53.1	247.5	0.21	72.5	0.1150	0.0022	5.2741	0.0965	0.3311	0.0033	0.1044	0.0051	1880	29	1865	16	98
JN2013-6-59	77.6	117.3	0.66	131.4	0.1010	0.0024	3.9284	0.0847	0.2821	0.0032	0.0887	0.0044	1643	44	1620	17	98
JN2013-6-60	176.9	173.8	1.02	41.6	0.1034	0.0024	4.0842	0.0926	0.2856	0.0031	0.0932	0.0050	1687	43	1651	19	96

Table 6 LA-ICP-MS zircon U–Pb data of Hujertu Formation (JN2013–8)

Sample Number	Content (ppm)		Th/U	Yb/Sm _N	Isotopic Elements Ratio				Age (Ma)				Concordance						
	Th	U			$^{207}\text{Pb}/^{235}\text{U}$	$^{206}\text{Pb}/^{238}\text{U}$	$^{206}\text{Pb}/^{232}\text{Th}$	$^{207}\text{Pb}/^{206}\text{Pb}$	$^{207}\text{Pb}/^{235}\text{U}$	$^{206}\text{Pb}/^{238}\text{U}$									
JN2013-8-01	367.4	258.8	1.42	36.8	0.0944	0.0023	3.4066	0.0804	0.2555	0.0031	0.0393	0.0005	1517	46	1506	19	1467	16	97
JN2013-8-02	86.4	104.9	0.82	154.5	0.1082	0.0036	4.8854	0.1570	0.3228	0.0014	0.0526	0.0014	1770	60	1800	27	1804	27	102
JN2013-8-04	316.4	326.0	0.97	86.6	0.0765	0.0019	2.1236	0.0520	0.1980	0.0023	0.0343	0.0005	1109	51	1157	17	1165	13	105
JN2013-8-07	139.3	406.8	0.34	104.8	0.0789	0.0014	2.2360	0.0407	0.2033	0.0020	0.0317	0.0007	1170	31	1192	13	1193	11	102
JN2013-8-08	108.3	217.4	0.50	84.2	0.0794	0.0019	2.2459	0.0532	0.2045	0.0023	0.0334	0.0007	1183	48	1196	17	1199	12	101
JN2013-8-10	110.3	149.3	0.74	53.3	0.1105	0.0025	4.8311	0.1046	0.3187	0.0042	0.0489	0.0008	1809	41	1790	18	1783	21	99
JN2013-8-11	131.3	110.2	1.19	22.9	0.1088	0.0031	4.5874	0.1438	0.3070	0.0047	0.0353	0.0007	1789	51	1747	26	1726	23	96
JN2013-8-12	97.5	76.7	1.27	46.5	0.1176	0.0032	5.4279	0.1568	0.3367	0.0051	0.0497	0.0009	1920	50	1889	25	1871	25	97
JN2013-8-13	69.8	97.0	0.72	91.5	0.0879	0.0027	3.0003	0.0959	0.2479	0.0031	0.0359	0.0007	1381	59	1408	24	1428	16	103
JN2013-8-14	144.6	122.7	1.18	74.9	0.0965	0.0023	3.8348	0.0975	0.2883	0.0034	0.0416	0.0006	1558	40	1600	20	1633	17	105
JN2013-8-16	253.1	60.3	4.19	36.2	0.1163	0.0032	5.2301	0.1310	0.3291	0.0041	0.0460	0.0005	1900	49	1858	21	1834	20	97
JN2013-8-17	139.1	135.7	1.02	107.3	0.0940	0.0025	3.5344	0.0864	0.2741	0.0035	0.0382	0.0007	1509	51	1535	19	1562	18	103
JN2013-8-18	273.5	325.5	0.84	96.6	0.1051	0.0016	4.2920	0.0687	0.2963	0.0032	0.0416	0.0005	1717	30	1692	13	1673	16	97
JN2013-8-23	135.4	181.0	0.75	73.0	0.0874	0.0020	2.9769	0.0760	0.2457	0.0029	0.0202	0.0003	1369	44	1402	19	1416	15	104
JN2013-8-25	74.7	162.7	0.46	113.2	0.0944	0.0025	3.3655	0.0947	0.2586	0.0041	0.0156	0.0003	1517	50	1496	22	1482	21	98
JN2013-8-27	56.0	186.4	0.30	130.9	0.1000	0.0020	4.0316	0.0786	0.2923	0.0033	0.0089	0.0002	1633	37	1641	16	1653	17	101
JN2013-8-34	99.4	70.9	1.40	68.2	0.0973	0.0031	3.7789	0.1326	0.2833	0.0061	0.0055	0.0001	1573	55	1588	28	1608	31	102
JN2013-8-35	311.0	277.1	1.12	35.8	0.0954	0.0019	3.4893	0.0764	0.2657	0.0046	0.0077	0.0001	1544	37	1525	17	1519	24	98
JN2013-8-36	149.8	159.8	0.94	94.3	0.0997	0.0023	3.8984	0.0887	0.2858	0.0055	0.0125	0.0002	1618	43	1613	18	1620	27	100
JN2013-8-37	121.3	176.1	0.69	92.5	0.0795	0.0024	2.3043	0.0729	0.2110	0.0036	0.0132	0.0002	1183	59	1214	22	1234	19	104
JN2013-8-38	246.4	498.8	0.49	14.1	0.1237	0.0016	6.2932	0.0960	0.3696	0.0061	0.0200	0.0003	2010	23	2018	13	2027	29	101
JN2013-8-39	66.8	134.6	0.50	95.8	0.1096	0.0027	4.8795	0.1216	0.3263	0.0066	0.0272	0.0005	1794	44	1799	21	1820	32	101
JN2013-8-40	181.7	362.0	0.50	34.5	0.0876	0.0015	2.8072	0.0521	0.2333	0.0043	0.0220	0.0003	1373	33	1357	14	1352	22	98
JN2013-8-41	123.8	90.7	1.37	71.8	0.1104	0.0034	4.9069	0.1833	0.3291	0.0103	0.0413	0.0007	1807	56	1803	32	1834	50	101
JN2013-8-42	148.5	167.9	0.88	24.4	0.0811	0.0021	2.3603	0.0663	0.2123	0.0046	0.0256	0.0006	1233	52	1231	20	1241	24	101
JN2013-8-43	93.6	91.7	1.02	89.5	0.0840	0.0036	2.4980	0.1183	0.2142	0.0050	0.0316	0.0008	1292	83	1271	34	1251	27	97
JN2013-8-44	185.3	214.6	0.86	108.2	0.1014	0.0019	4.3387	0.0981	0.3097	0.0064	0.0445	0.0006	1650	33	1701	19	1739	32	105
JN2013-8-45	102.5	165.2	0.62	40.8	0.0780	0.0019	2.0158	0.0627	0.1868	0.0043	0.0290	0.0007	1148	50	1121	21	1104	23	96
JN2013-8-47	138.0	149.1	0.93	50.3	0.1161	0.0020	5.5609	0.1192	0.3460	0.0071	0.0539	0.0007	1898	31	1910	18	1916	34	101
JN2013-8-48	78.0	155.3	0.50	42.9	0.0785	0.0019	2.2208	0.0692	0.2045	0.0058	0.0345	0.0007	1158	47	1188	22	1199	31	104
JN2013-8-49	43.1	109.6	0.39	164.6	0.0882	0.0031	2.8972	0.1106	0.2382	0.0060	0.0397	0.0014	1387	68	1381	29	1378	31	99
JN2013-8-50	109.2	127.6	0.86	62.4	0.0834	0.0022	2.5903	0.0841	0.2257	0.0062	0.0379	0.0009	1277	48	1298	24	1312	33	103
JN2013-8-52	133.3	113.6	1.17	27.8	0.1685	0.0032	11.5782	0.2964	0.5003	0.0134	0.0794	0.0012	2542	31	2571	24	2615	58	103
JN2013-8-53	112.7	56.5	1.99	80.4	0.0816	0.0036	2.2509	0.1089	0.2035	0.0071	0.0334	0.0008	1236	86	1197	34	1194	38	97
JN2013-8-54	150.5	173.7	0.87	30.7	0.0940	0.0023	3.3743	0.1011	0.2609	0.0064	0.0465	0.0011	1509	46	1498	23	1494	33	99
JN2013-8-55	85.9	104.2	0.82	123.7	0.0922	0.0026	3.4012	0.1142	0.2708	0.0078	0.0480	0.0010	1472	54	1505	26	1545	40	105
JN2013-8-56	151.9	212.2	0.72	87.5	0.0960	0.0020	3.6625	0.0966	0.2800	0.0073	0.0461	0.0009	1548	39	1563	21	1591	37	103
JN2013-8-57	99.3	95.4	1.04	76.9	0.0891	0.0032	2.7993	0.1016	0.2361	0.0072	0.0437	0.0012	1406	37	1355	27	1366	38	97
JN2013-8-58	67.9	90.3	0.75	175.4	0.0950	0.0025	3.6636	0.1138	0.2836	0.0078	0.0488	0.0010	1528	50	1563	25	1610	39	105
JN2013-8-59	331.9	208.3	1.59	50.3	0.0942	0.0023	3.1742	0.1036	0.2503	0.0082	0.0415	0.0006	1522	51	1451	25	1440	42	95
JN2013-8-60	128.8	178.1	0.72	101.2	0.0759	0.0024	1.8599	0.0627	0.1826	0.0048	0.0324	0.0006	1092	63	1067	22	1081	26	99

generally comparable with the Qingbaikou period (1000–800 Ma) (Li et al., 2013).

5.2 NCC provenance

The age of detrital zircons in Bayan Obo Group can be divided into the following groups: 2.51–2.71 Ga, 2.00–2.48 Ga, 1.95–1.80 Ga, 1.60–1.75 Ga and 1.10–1.60 Ga. The zircons with ages of Neo–Archean (2.51–2.71 Ga) and early Paleoproterozoic (2.00–2.48 Ga) are mainly present in Dulahala, Jianshan and Halahuogete Formation, especially there exists a prominent peak of this age range in Halahuogete Formation. The Th/U ratio for most of zircons falling into this age range is larger than 0.1, which indicates they are magmatic, but oscillatory zones of some zircons are really weak implying they were metamorphic zircons affected by recrystallization. The magmatism and metamorphism in the period of 2.60–2.58 Ga and 2.52–2.48 Ga have been reported in Yinshan Block (Ma et al., 2018). For example, the 2535±8 Ma diorite in the Guyang area (Ma et al., 2018), 2697±11 Ma granitic gneiss in the Xi Ulanbulang area (Dong et al., 2012b), 2502±14 Ma hornblende, 2581±7 Ma gneissic granite and 2479±21 Ma kyanite–garnet–bearing monzogranitic gneiss (Wang et al., 2015), 2511±11 Ma mate–gabbro, 2512±10 Ma charnockite (Zhang X H et al., 2014), protolith age of amphibolite is at 2538±9 Ma and its metamorphism age at 2452±7 Ma in Guyang area (Ma X D et al., 2014), 2465±18 Ma tonalite, 2523±7 Ma diorite (Ma et al., 2013), 2503±10 Ma hornblende monzogranulite and 2472±14 Ma biotite monzogranulite in Xi Ulan area (Dong et al., 2012a). At the same time, in the eastern part of the Khondalite Belt, such as Zhuozhi area, the detrital zircons in sillimanite–cordierite–garnet gneiss yield weighted mean age at 2017±9 Ma (Cai et al., 2017), and the detrital zircons from garnet–bearing felsic gneiss gave peak age of 2040 Ma (Jiao et al., 2013). The peak age of the cordierite–garnet–sillimanite gneiss in the Jining complex is 2086 Ma (Xia et al., 2006). Therefore, the magmatic rocks and metamorphic rocks existing in the area of Guanyang, Xi Ulanbulang and Zhuozhi might provide the detritus with age of Neoproterozoic and early paleoproterozoic for Bayan Obo Group. This conclusion is also consistent with paleocurrent from southwest to northeast during the deposition of Jianshan Formation (Zhang X, 2014).

The detrital zircons with age from 1.95 Ga to 1.80 Ga mainly occurred in the Dulahala and Jianshan Formation, and there only existed a small amount of zircons with this age in the middle and upper succession of Bayan Obo Group. Th/U ratio of zircons falling into this age range is larger than 0.1, which is not typical for metamorphic zircons. However, zircons underwent granulite facies metamorphism could have a very high Th/U ratio. Meanwhile, the CL images of these zircons also show metamorphic characteristics, therefore zircons with age from 1.95 Ga to 1.80 Ga are mainly metamorphic. 1.95–1.80 Ga metamorphism are widespread in the Khondalite Belt. For example, in Zhuozhi area, 1945±15 Ma, 1902±16 Ma and 1842±20 Ma sillimanite–garnet gneisses (Xia et al., 2006), 1919±10 Ma granulite (Santosh et al., 2007) and the garnet–bearing quartz lens with age of 1896±4 Ma, 1916±6 Ma and 1891±5 Ma were reported (Jiao et al.,

2013). In Daqingshan area, the metamorphic zircons from gneiss yielded ~1.90 Ga metamorphic age (Ma et al., 2015), tonalitic gneiss and charnockitic gneiss gave the metamorphic ages at 1904±13 Ma and 1936±20 Ma, respectively. The metamorphic zircons obtained from mylonitized charnockite yielded ages ranging from 1846 Ma to 1945 Ma (Liu J H et al., 2017), and metamorphic zircons from amphibolite yielded weighted mean age at 1941±14 Ma and 1910±9 Ma (Wang X et al., 2018). It is worth noting that the HREE form of zircon in garnet–bearing metamorphic rocks will be much flatter (Schaltegger et al., 1999; Whitehouse et al., 2003), but the metamorphic zircons formed under granulite facies through anatexis could show a HREE form similar to that of magmatic zircons. Under this situation, the formation of garnets will not affect the HREE content (Rubatto, 2002). The gneiss and garnet–bearing felsic gneiss in Daqingshan area show characteristics of anatexis (Ma et al., 2015; Xu et al., 2015), the Yb/Sm_N of almost all 1.95–1.80 Ga detrital zircons in this study is more than 10 (Table 1-6), therefore, the Daqingshan and Zhuozhi areas in the Khondalite Belt may be the main provenances for the late Paleoproterozoic zircons.

1.60–1.75 Ga detrital zircons mainly occurred in the Bilute, Baiyinbaolage and Hujiertu Formation. Most of these zircons develop oscillatory zone with Th/U ratio larger than 0.1, implying they are magmatic. The magmatic events of this age are widespread in NCC, such as the AMCG assemblage and the mafic dykes formed in the post–collision extensional environment after convergence of eastern and western landmasses at 1.85 Ga. The mafic dykes are mainly distributed in Taihang–Lvliang area with ages of 1769–1778 Ma (Wang et al., 2004; Peng et al., 2007; Peng et al., 2012). There are AMCG assemblages in Miyun area, such as the 1715±6 Ma and 1693±7 Ma plagioclase in Damiao, Hebei (Zhao et al., 2004a), 1692–1753 Ma Changsaoying and Gubeikou moyite and syenite (Zhang et al., 2007), 1790–1614 Ma Shachang biotite granite (Wang X X et al., 2018), ~1679 Ma Wenquan A type granite (Jiang et al., 2011), the 1696–1721 Ma Jianping diorite and syenite (Wang W et al., 2013), 1679–1685 Ma rapakivi granite in Miyun area (Peng et al., 2012; Gao et al., 2008; Yang et al., 2005). Because the mafic rocks contain small amount of zircons and their mineral composition is dominated by easily weatherable mafic minerals, they are not regarded as the provenance of the Bayan Obo Group. Therefore, the granitic rocks in Miyun area may be the main provenances for the detrital zircons with age of 1.60–1.75 Ga in Bayan Obo Group.

Combined with previous published ages of detrital zircons, it can be found that the provenances of the Bayan Obo group show a regular change during the period of its sedimentation (Fig. 8). The ages of detrital zircons from Dulahala Formation show a dominant peak at 1960 Ma and a weaker peak at 2520 Ma. Jianshan Formation shows two dominant peaks at 1920 Ma and 2540 Ma. It should be noted that the age peaks of 2.50–2.70 Ga in the two formations are comparably weak, indicating that the Khondalite Belt was the dominant provenance while Yinshan Block served as the secondary provenance.

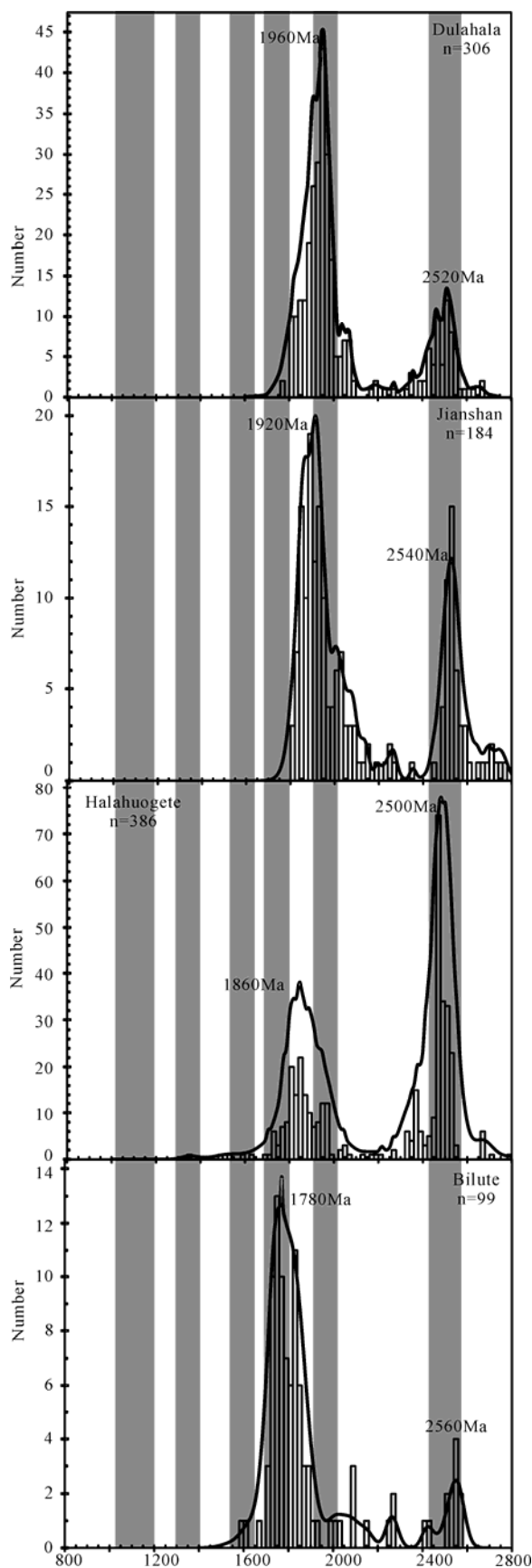


Fig. 8. Binned frequency histograms of Dulahala, Jianshan, Halahuogete and Bilute formations from Bayan Obo Group. Data source from Zhong et al., (2015); Zhou et al., (2016); Liu C H et al., (2017); Zhou et al., (2018).

Halahuogete Formation yields two main age peaks at 1860 Ma and 2500 Ma, Bilute Formation shows a major age peak at 1780 Ma and a minor age peak at 2560 Ma. The age peak of 2.50–2.70 Ga in Halahuogete Formation is more prominent than that in Dulahala and Jianshan Formation, which might imply the erosion rate of the basement in Yinshan Block come to peak at ~1600 Ma and it therefore became the dominant provenance for Halahuogete Formation. For the Bilute Formation, the Khondalite Belt was still its main provenance, and the supply of 2460 Ma detrital material from the Yinshan Block was relatively weak. In Baiyinbaolage and Huijiertu Formation, the upper part of Bayan Obo Group, there exist age peaks younger than 1.60 Ga, which indicates a non-NCC provenance for them. The details will be discussed in the following part.

5.3 Non-NCC provenance

According to previous studies about provenances of the Meso-proterozoic sedimentary strata in the northern margin of the North China Craton, it was believed that these zircons with age younger than 1.60 Ga might come from North American, Baltic, North Indian or Australia (Liu et al., 2014; Liu C H et al., 2017; Liu et al., 2018). And the fact that there is no 1.58–1.53 Ga magmatism in the Laurentia (Aleinikoff et al., 2013) made it impossible to be provenance for the detrital zircons with the same ages in Bayan Obo Group. On Baltic developed magmatism of 1.59–1.48 Ga, 1.37–1.33 Ga and 1.18–1.08 Ga (Åhäll et al., 2000), making it the potential provenance for the Bayan Obo Group (Liu C H et al., 2017). However, the hypothesis that NCC remained closed to Baltic during the whole-time span from 1.55 Ga to 0.9 Ga needs further consideration.

In recent years, the palaeogeographic location of NCC from the early Mesoproterozoic to Neoproterozoic has also been a hot topic (Li et al., 1996; Zhang et al., 2006; Zhang et al., 2009; Zhai et al., 2011a; Zhang et al., 2012; Zhang et al., 2017). ~1.32 Ga mafic rocks and bimodal volcanic rocks developed in the northern margin of NCC indicated that the northern and southern margin of NCC were adjacent to Laurentia and Siberia respectively from early Paleoproterozoic to middle Mesoproterozoic (Zhang et al., 2009; Zhang et al., 2012). The ~1.32 Ga large igneous province in the northern margin of NCC indicated that the northern and northeastern margins of NCC were likely to be adjacent to the northern margin of the northern Australia during 1.6–1.5 Ga, and the separation was at around 1.33 Ga (Zhang et al., 2017). Based on paleomagnetic data, NCC and Laurentia shared the similar APWPs between 1200–700 Ma, indicating that the two cratons were adjacent to each other in Rodinia, and the separation of them commenced at 650–615 Ma (Li et al., 1996; Zhang et al., 2006). More paleomagnetic data obtained in recent years also supported the proximities among NCC, Laurentia, Siberia and Baltic in the early Mesoproterozoic to Neoproterozoic, and the separation of NCC from Columbia might begin at ~1400 Ma (Xu et al., 2014; Fu et al., 2015).

In most supercontinent reconstruction models, the northwestern part of Baltic was connected to the eastern

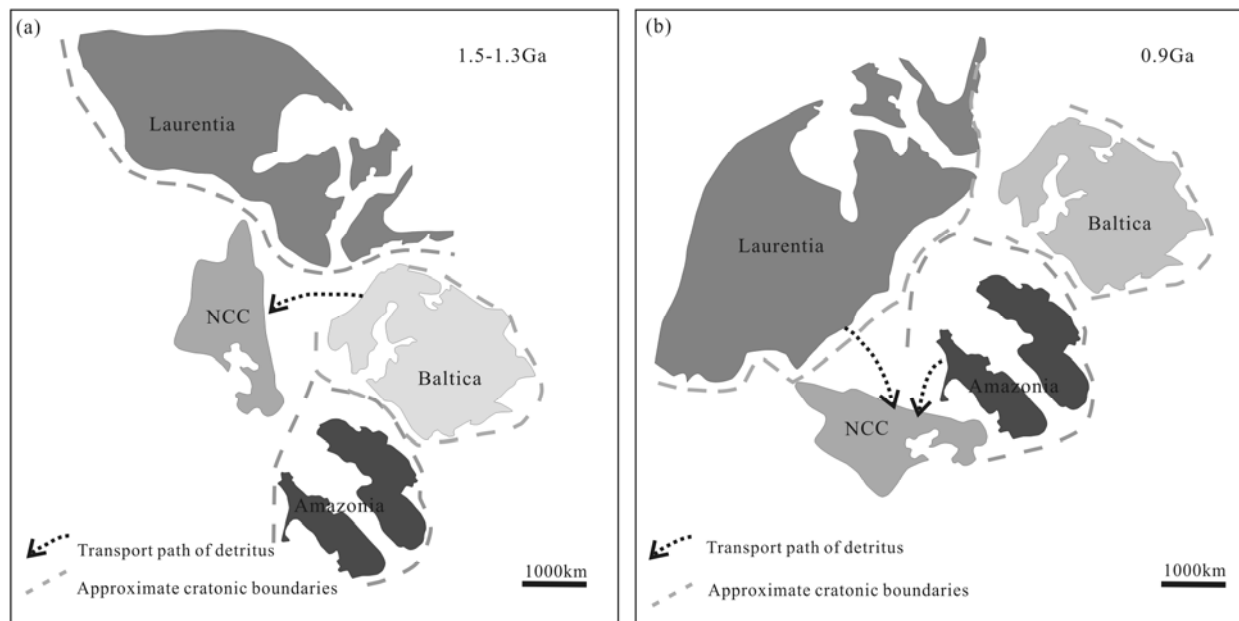


Fig. 9. The provisional connection among NCC, Baltic, Amazonia and Laurentia during 1.5–1.3 Ga and 0.9 Ga based on the SAMBA hypothesis (Johansson, 2009).

The black dotted arrow lines represent the possible transportation path of detritus from other cratons to NCC.

part of Laurentia from 1.9 Ga to 1.3 Ga (Johansson, 2009). The SAMBA model (South America–Baltic) of Rodinia connected the northwest Amazonia to the southwest Baltic and the western margin of Baltic collided with southeastern margin of Amazonia at 0.9–1.1 Ga (Johansson, 2009). Cawood et al. (2017) also suggested that with the final closure of the Mirovoi Ocean, the western Amazonia collided with the eastern Laurentia at 1.0 Ga. At the same time, the southern margin of Baltic collided with the northern Amazonia, forming a part of the Rodinia. Therefore, Amazonia and Baltic were placed adjacent to each other in these models. What's more, magmatism with ages of 1.78–1.55 Ga, 1.50–1.30 Ga and 1.25–1.10 Ga developed in Rondonian–San Ignacio Province of Amazonia (Bettencourt et al., 2010), which will serve as a potential provenance for the detrital zircons with ages younger than 1.60 Ga in Bayan Obo Group.

Based on the Rodinia reconstruction model proposed by predecessors and the age of detrital zircons obtained from Bayan Obo Group in this paper, it is believed that during 1560–1350 Ma, when Bilute Formation deposited, Baltic was potential non–NCC provenance. When Baiyinbaolage and Hujertu Formation deposited, Amazonia and Laurentia might provide detrital zircons younger than 1.60 Ga. Therefore, NCC might be more adjacent to Amazonia and Laurentia in Rodinia (Fig. 9).

6 Conclusions

Based on the studies on ages of detrital zircons from Bayan Obo Group, this paper mainly discussed its provenances and the position of NCC in Rodinia, and came to these following conclusions:

The deposition time of the Dulahala and Jianshan

Formation was 1.80–1.65 Ga, Halahuogete and the Bilute Formation was 1.56–1.35 Ga, and Baiyinbaolage and Hujertu Formation was 1250–900 Ma.

Detrital zircons with age of 2.51–2.71 Ga and 2.00–2.48 Ga were from Guyang, Xi Ulanbulang and Zhuozi area; the Khondalite Belt provided detrital zircons with age of 1.95–1.80 Ga; zircons with age of 1.60–1.75 Ga might come from granitic rocks in Miyun Area.

Baltic might provide the detrital zircons with ages younger than 1.60 Ga for Bilute Formation during 1560–1350 Ma, while Amazonia and Laurentia provided detrital zircons younger than 1.60 Ga in Baiyinbaolage and Hujertu Formation, suggesting that NCC might be adjacent to Amazonia and Laurentia in Rodinia.

Acknowledgements

We thank two anonymous reviewers for their constructive and thorough reviews that helped us improve the paper. This research is financially supported by the National Natural Science Foundation of China (No.41872203), China Geological Survey (No.1212011120709) and Doctoral Candidate Inter Discipline Fund of Jilin University (No.10183201837).

Manuscript received May 15, 2019
accepted Aug. 14, 2019
associate EIC XIAO Wenjiao
edited by LIU Lian

References

- Åhäll, K.I., and Connelly, J., 1998. Intermittent 1.53–1.13Ga magmatism in western Baltica; age constraints and correlations within a postulated supercontinent. *Precambrian Research*, 92(1): 1–20.

- Åhäll, K.I., Connelly, J.N., and Brewer, T.S., 2000. Episodic rapakivi magmatism due to distal orogenesis?: Correlation of 1.69–1.50 Ga orogenic and inboard, “anorogenic” events in the Baltic Shield. *Geology*, 28(9): 823–826.
- Aleinikoff, J.N., Southworth, S., and Merschat, A.J., 2013. Implications for late Grenvillian (Rigolet phase) construction of Rodinia using new U–Pb data from the Mars Hill terrane, Tennessee and North Carolina, United States. *Geology*, 41(10): 1087–1090.
- Andersen, T., 2002. Correction of common lead in U–Pb analyses that do not report ^{204}Pb . *Chemical Geology*, 192(1–2): 59–79.
- Bettencourt, J.S., Leite, W.B., Ruiz, A.S., Matos, R., Payolla, B.L., and Tosdal, R.M., 2010. The Rondonian–San Ignacio Province in the SW Amazonian Craton: An overview. *Journal of South American Earth Sciences*, 29(1): 28–46.
- Cai, J., Liu, F.L., and Liu, P.H., 2017. Paleoproterozoic multistage metamorphic events in Jining metapelitic rocks from the Khondalite Belt in the North China Craton: Evidence from petrology, phase equilibria modelling and U–Pb geochronology. *Journal of Asian Earth Sciences*, 138: 515–534.
- Campbell, L.S., Compston, W., Sircombe, K.N., and Wilkinson, C.C., 2014. Zircon from the East Orebody of the Bayan Obo Fe–Nb–REE deposit, China, and SHRIMP ages for carbonatite-related magmatism and REE mineralization events. *Contributions to Mineralogy and Petrology*, 168: 1–23.
- Cawood, P.A., and Pisarevsky, S.A., 2017. Laurentia–Baltica–Amazonia relations during Rodinia assembly. *Precambrian Research*, 292, 386–397.
- CorreaGomes, L.C., and Oliveira, E.P., 2000. Radiating 1.0 Ga mafic dyke swarms of eastern Brazil and western Africa: Evidence of post-assembly extension in the rodinia supercontinent? *Gondwana Research*, 3: 325–332.
- Dalziel, I.W.D., 1991. Pacific margins of Laurentia and East Antarctica–Australia as a conjugate rift pair: Evidence and implications for an Eocambrian supercontinent. *Geology*, 19: 598–601.
- Dalziel, I.W.D., Mosher, S., and Gahagan, L.M., 2000. Laurentia–Kalahari collision and the assembly of Rodinia. *Journal of Geology*, 108: 499–513.
- Dong, X.J., Xu, Z.Y., Liu, Z.H., and Sha, Q., 2012a. Zircon U–Pb geochronology of Archean high-grade metamorphic rocks from Xi Ulanbulang area, central Inner Mongolia. *Science China Earth Sciences*, 55: 204–212.
- Dong, X.J., Xu, Z.Y., Liu, Z.H., and Sha, Q., 2012b. 2.7 Ga granitic gneiss in the northern foot of Daqingshan mountain, central Inner Mongolia, and its geological implications. *Diqiu Kexue–Zhongguo Dizhi Daxue Xuebao/Earth Science–Journal of China University of Geosciences*, 37:20–27 (in Chinese with English abstract).
- Eggins, S.M., Kinsley, L.P.J., and Shelley, J.M.G., 1998. Deposition and element fractionation processes during atmospheric pressure laser sampling for analysis by ICP–MS. *Applied Surface Science*, 127–129: 278–286.
- Evans, D.A.D., and Mitchell, R.N., 2011. Assembly and breakup of the core of Paleoproterozoic–Mesoproterozoic supercontinent Nuna. *Geology*, 39: 443–446.
- Evans, D.A.D., 2013. Reconstructing pre–Pangean supercontinents. *GSA Bulletin*, 125: 1735–1751.
- Fu, X.M., Zhang, S.H., Li, H.Y., Ding, J.K., Li, H.K., Yang, T.S., Wu, H.C., Yuan, H.F., and Lv, J., 2015. New paleomagnetic results from the Huaibei Group and Neoproterozoic mafic sills in the North China Craton and their paleogeographic implications. *Precambrian Research*, 269: 90–106.
- Gao, L.Z., Liu, P.J., Yin, C.Y., Zhang, C.H., Ding, X.Z., Liu, Y.X., and Song, B., 2011. Detrital Zircon Dating of Meso–and Neoproterozoic Rocks in North China and Its Implications. *Acta Geologica Sinica (English Edition)*, 85(2): 271–282.
- Gao, W., Zhang, C.H., Gao, L.Z., and Shi, X.Y., 2008. Zircon SHRIMP U–Pb age of rapakivi granite in Miyun, Beijing, and its tectono–stratigraphic implications. *Geological Bulletin of China*, 27(6): 793–798 (in Chinese with English abstract).
- Gong, W.B., Hu, J.M., Li, Z.H., Dong, X.P., Liu, Y., and Liu, S.C., 2016. Detrital zircon U–Pb dating of Zhaertai Group in the North Margin Rift Zone of North China Craton and its implications. *Acta Petrologica Sinica*, 32(7): 2151–2165 (in Chinese with English abstract).
- Hawkesworth, C.J., and Cawood, P.A., 2014. Earth’s middle age. *Geology*, 42(6): 503–506.
- Hoffman, P.F., 1991. Did the breakout of Laurentia turn Gondwanaland inside–out? *Science*, 252(5011): 1409–1412.
- Hu, B., Zhai, M., Guo, J., Peng, P., Liu, F., and Liu, S., 2009. LA–ICP–MS U–Pb geochronology of detrital zircons from the Huade Group in the northern margin of the North China Craton and its tectonic significance. *Acta Petrologica Sinica*, 25(1): 193–211 (in Chinese with English abstract).
- Hu, J.M., Gong, W.B., Wu, S.J., Liu, Y., and Liu, S.C., 2014. LA–ICP–MS zircon U–Pb dating of the Langshan Group in the northeast margin of the Alxa block, with tectonic implications. *Precambrian Research*, 255: 756–770.
- Hu, J.M., Gong, W.B., Zhao, Y., Zhang, S.H., Wu, S.J., Qu, H.J., Li, Z.H., and Liang, X., 2015. The Confirmation of the Neoproterozoic Langshan Group in Inner Mongolia and Its Significance. *Acta Geologica Sinica (English Edition)*, 89(1): 318–319.
- Jackson, S.E., Pearson, N.J., Griffin, W.L., and Belousova, E.A., 2004. The application of laser ablation–inductively coupled plasma–mass spectrometry to in situ U–Pb zircon geochronology. *Chemical Geology*, 211(1): 47–69.
- Jiang, N., Guo, J.H., and Zhai, M.G., 2011. Nature and origin of the Wenquan granite: Implications for the provenance of Proterozoic A–type granites in the North China craton. *Journal of Asian Earth Sciences*, 42(1): 76–82.
- Jiao, S.J., Guo, J.H., Harley, S.L., and Peng, P., 2013. Geochronology and trace element geochemistry of zircon, monazite and garnet from the garnetite and/or associated other high-grade rocks: Implications for Palaeoproterozoic tectonothermal evolution of the Khondalite Belt, North China Craton. *Precambrian Research*, 237: 78–100.
- Johansson, Å., 2009. Baltica, Amazonia and the SAMBA connection–1000 million years of neighbourhood during the Proterozoic? *Precambrian Research*, 175(1): 221–234.
- Karlstrom, K.E., Harlan, S.S., Williams, M.L., McLelland, J., Geissman, J.W., and Åhäll, K.I., 1999. Refining Rodinia: Geologic evidence for the Australia–Western U.S. Connection in the Proterozoic. *GSA Today*, 9(10): 2–7.
- Kusky, T.M., and Santosh, M., 2009. The Columbia connection in North China. *Geological Society Special Publication*, 323: 49–71.
- Li, H.K., Zhu, S.X., Xiang, Z.Q., and Su, W.B., 2010. Zircon U–Pb dating on tuff bed from Gaoyuzhuang Formation in Yanqing, Beijing: Further constraints on the new subdivision of the Mesoproterozoic stratigraphy in the northern North China Craton. *Acta Petrologica Sinica*, 26(7): 2131–2140 (in Chinese with English abstract).
- Li, H.K., Lu, S.N., Su, W.B., Xiang, Z.Q., Zhou, H.Y., and Zhang, Y.Q., 2013. Recent advances in the study of the Mesoproterozoic geochronology in the North China Craton. *Journal of Asian Earth Sciences*, 72: 216–227.
- Li, H.K., Su, W.B., Zhou, H.Y., and Xiang, Z.Q., 2014. The first precise age constraints on the Jixian System of the Meso– to Neoproterozoic Standard Section of China: SHRIMP zircon U–Pb dating of bentonites from the Wumishan and Tieling formations in the Jixian Section, North China Craton. *Acta Petrologica Sinica*, 30(10): 2999–3012 (in Chinese with English abstract).
- Li, Q.L., Chen, F., Guo, J.H., Li, X.H., Yang, Y.H., and Siebel, W., 2007. Zircon ages and Nd–Hf isotopic composition of the Zhaertai Group (Inner Mongolia): Evidence for early Proterozoic evolution of the northern North China Craton. *Journal of Asian Earth Sciences*, 30(3–4): 573–590.
- Li, Z.X., Zhang, L., and Powell, C.M., 1996. Positions of the East Asian cratons in the Neoproterozoic supercontinent Rodinia. *Australian Journal of Earth Sciences*, 43(6): 593–604.
- Li, Z.X., Bogdanova, S.V., Collins, A.S., Davidson, A., De Waele, B., Ernst, R.E., Fitzsimons, I.C.W., Fuck, R.A., Gladkochub, D.P., Jacobs, J., Karlstrom, K.E., Lu, S., Natapov, L.M., Pease, V., Pisarevsky, S.A., Thrane, K., and

- Vernikovsky, V., 2008. Assembly, configuration, and break-up history of Rodinia: A synthesis. *Precambrian Research*, 160 (1): 179–210.
- Liu, C.H., Zhao, G.C., and Liu, F.L., 2014. Detrital zircon U–Pb, Hf isotopes, detrital rutile and whole-rock geochemistry of the Huade Group on the northern margin of the North China Craton: Implications for the breakup of the Columbia supercontinent. *Precambrian Research*, 254: 290–305.
- Liu, C.H., Zhao, G.C., Liu, F.L., and Shi, J.R., 2017. Detrital zircon U–Pb and Hf isotopic and whole-rock geochemical study of the Bayan Obo Group, northern margin of the North China Craton: Implications for Rodinia reconstruction. *Precambrian Research*, 303: 372–391.
- Liu, J.H., Liu, F.L., Ding, Z.J., Liu, P.H., Chen, J.Q., Liu, C.H., Wang, F., Yang, H., Cai, J., and Shi, J.R., 2017. Late Neoproterozoic–Paleoproterozoic arc–continent accretion along the Khondalite Belt, Western Block, North China Craton: Insights from granitoid rocks of the Daqingshan–Wulashan area. *Precambrian Research*, 303: 494–519.
- Liu, X.G., Li, S.Z., Li, X.Y., Zhao, S.J., Wang, T.S., Yu, S.Y., Dai, L.M., Zhou, Z.Z., and Guo, R.H., 2018. Detrital zircon U–Pb geochronology and provenance of the Sanxiatian Formation (Huade Group) in the North China Craton: Implications for the breakup of the Columbia supercontinent. *Precambrian Research*, 310: 305–319.
- Liu, Y.S., Gao, S., Hu, Z.C., Gao, C.G., Zong, K.Q., and Wang, D.B., 2009. Continental and Oceanic Crust Recycling–induced Melt–Peridotite Interactions in the Trans–North China Orogen: U–Pb Dating, Hf Isotopes and Trace Elements in Zircons from Mantle Xenoliths. *Journal of Petrology*, 51(1–2): 537–571.
- Liu, Y.S., Hu, Z.C., Zong, K.Q., Gao, C.G., Gao, S., Xu, J., and Chen, H.H., 2010. Reappraisal and refinement of zircon U–Pb isotope and trace element analyses by LA–ICP–MS. *Chinese Science Bulletin*, 55(15): 1535–1546.
- Lu, S.N., Yang, C.L., Li, H.K., and Li, H.M., 2002. A group of rifting events in the terminal paleoproterozoic in the North China craton. *Gondwana Research*, 5(1): 123–131.
- Lu, S.N., Zhao, G.C., Wang, H.C., and Hao, G.J., 2008. Precambrian metamorphic basement and sedimentary cover of the North China Craton: A review. *Precambrian Research*, 160 (1): 77–93.
- Ludwig, K.R., 2003. *Isoplot 3.09—A Geochronological Toolkit for Microsoft Excel*. Berkeley Geochronology Center Special Publication: 1–4.
- Ma, M.Z., Zhang, Y.X., Xie, H.Q., and Wan, Y.S., 2014. SHRIMP U–Pb dating and LA–ICPMS Hf isotope analysis of detrital zircons from medium–to coarse–grained sandstones of the Bayan Obo Group and Sailinhuodong Group and its geological significances. *Acta Petrologica Sinica*, 30(10): 2973–2988 (in Chinese with English abstract).
- Ma, M.Z., Dong, C.Y., Xu, Z.Y., and Xie, S.W., 2015. Anatexis of Early Paleoproterozoic garnet–biotite gneisses (Daqingshan supracrustal rocks) in Daqingshan, Inner Mongolia: Geology, zircon geochronology and geochemistry. *Acta Petrologica Sinica*, 31(6): 1535–1548 (in Chinese with English abstract).
- Ma, X.D., Guo, J.H., Liu, F., Qian, Q., and Fan, H.R., 2013. Zircon U–Pb ages, trace elements and Nd–Hf isotopic geochemistry of Guyang sanukitoids and related rocks: Implications for the Archean crustal evolution of the Yinshan Block, North China Craton. *Precambrian Research*, 230: 61–78.
- Ma, X.D., Fan, H.R., Santosh, M., and Guo, J.H., 2014. Chronology and geochemistry of Neoproterozoic BIF–type iron deposits in the Yinshan Block, North China Craton: Implications for oceanic ridge subduction. *Ore Geology Reviews*, 63: 405–417.
- Ma, X.D., and Zhong, Y., 2018. Geochemistry and chronology of a diorite pluton in the Yinshan Block, implications for crustal growth and evolution of North China Craton. *Geological Journal*, 53(6): 2849–2862.
- Moore, E.M., 1991. Southwest U.S.–East Antarctic (SWEAT) connection: A hypothesis. *Geology*, 19(5): 425–428.
- Peng, P., Zhai, M.G., Guo, J.H., Kusky, T.M., and Zhao, T.P., 2007. Nature of mantle source contributions and crystal differentiation in the petrogenesis of the 1.78 Ga mafic dykes in the central North China craton. *Gondwana Research*, 12(1): 29–46.
- Peng, P., Bleeker, W., Ernst, R.E., Söderlund, U., and McNicoll, V., 2011a. U–Pb baddeleyite ages, distribution and geochemistry of 925Ma mafic dykes and 900Ma sills in the North China craton: Evidence for a Neoproterozoic mantle plume. *Lithos*, 127(1): 210–221.
- Peng, P., Zhai, M.G., Li, Q.L., Wu, F.Y., Hou, Q.L., Li, Z., Li, T.H., and Zhang, Y.B., 2011b. Neoproterozoic (~900Ma) Sariwon sills in North Korea: Geochronology, geochemistry and implications for the evolution of the south–eastern margin of the North China Craton. *Gondwana Research*, 20(1): 243–254.
- Peng, P., Liu, F., Zhai, M.G., and Guo, J.H., 2012. Age of the Miyun dyke swarm: Constraints on the maximum depositional age of the Changcheng System. *Chinese Science Bulletin*, 57 (1): 105–110 (in Chinese with English abstract).
- Peng, P., 2015. Precambrian mafic dyke swarms in the North China Craton and their geological implications. *Science China Earth Sciences*, 58(5): 649–675 (in Chinese with English abstract).
- Piper, J.D.A., 1982. The Precambrian palaeomagnetic record: the case for the Proterozoic Supercontinent. *Earth and Planetary Science Letters*, 59(1): 61–89.
- Piper, J.D.A., 2000. The Neoproterozoic Supercontinent: Rodinia or Palaeopangaea? *Earth and Planetary Science Letters*, 176 (1): 131–146.
- Pulsipher, M.A., and Dehler, C.M., 2019. U–Pb detrital zircon geochronology, petrography, and synthesis of the middle Neoproterozoic Visingsö Group, Southern Sweden. *Precambrian Research*, 320: 323–333.
- Qiao, X.F., Yao, P.Y., Wang, C.S., and Lin, T., 1991. Sequence Stratigraphy and Tectonic Environment of the Chartai Group, Inner Mongolia. *Acta Geologica Sinica (English Edition)*, 4 (3): 217–235.
- Qiao, X.F., and Wang, Y.B., 2014. Discussions on the lower boundary age of the Mesoproterozoic and basin tectonic evolution of the Mesoproterozoic in North China Craton. *Acta Geologica Sinica (English Edition)*, 88(9): 1623–1637 (in Chinese with English abstract).
- Rogers, J.J.W., 1996. A history of continents in the past three billion years. *The Journal of Geology*, 104(1): 91.
- Rogers, J.J.W., and Santosh, M., 2002. Configuration of Columbia, a mesoproterozoic supercontinent. *Gondwana Research*, 5(1): 5–22.
- Rubatto, D., 2002. Zircon trace element geochemistry: partitioning with garnet and the link between U–Pb ages and metamorphism. *Chemical Geology*, 184(1): 123–138.
- Santosh, M., Wilde, S.A., and Li, J.H., 2007. Timing of Paleoproterozoic ultrahigh–temperature metamorphism in the North China Craton: Evidence from SHRIMP U–Pb zircon geochronology. *Precambrian Research*, 159(3–4): 178–196.
- Santosh, M., 2010. Assembling North China Craton within the Columbia supercontinent: The role of double–sided subduction. *Precambrian Research*, 178(1–4): 149–167.
- Schaltegger, U., Fanning, C.M., Günther, D., Maurin, J.C., Schulmann, K., and Gebauer, D., 1999. Growth, annealing and recrystallization of zircon and preservation of monazite in high–grade metamorphism: conventional and in–situ U–Pb isotope, cathodoluminescence and microchemical evidence. *Contributions to Mineralogy and Petrology*, 134(2): 186–201.
- Shi, Y.R., Liu, D.Y., Kröner, A., Jian, P., Miao, L.C., and Zhang, F.P., 2012. Ca. 1318Ma A–type granite on the northern margin of the North China Craton: Implications for intraplate extension of the Columbia supercontinent. *Lithos*, 148: 1–9.
- Smethurst, M.A., Khramov, A.N., and Torsvik, T.H., 1998. The Neoproterozoic and Palaeozoic palaeomagnetic data for the Siberian Platform: From Rodinia to Pangea. *Earth-Science Reviews*, 43(1): 1–24.
- Sun, S.F., 1992. New discovery of fossil microplants in the Jianshan Formation of Bayan Obo Group, Inner Mongolia. *Geological Review*, 38: 474–482 (in Chinese with English abstract).
- Su, W.B., Li, H.K., Huff, W.D., Ettensohn, F.R., Zhang, S.H.,

- Zhou, H.Y., and Wan, Y.S., 2010. SHRIMP U–Pb dating for a K–bentonite bed in the Tieling Formation, North China. *Chinese Science Bulletin*, 55(29): 3312–3323 (in Chinese with English abstract).
- Tan, L.K., and Shi, T.Z., 2000. Discovery and Significance of Small Shelly Fossils in the Bayan Obo Group in Shangdu, Inner Mongolia. *Geological Review*, 46: 573–584 (in Chinese with English abstract).
- Wang, D., Guo, J.H., Huang, G.Y., and Scheltens, M., 2015. The Neoproterozoic ultramafic–mafic complex in the Yinshan Block, North China Craton: Magmatic monitor of development of Archean lithospheric mantle. *Precambrian Research*, 270: 80–99.
- Wang, W., Liu, S.W., Bai, X., Li, Q.G., Yang, P.T., Zhao, Y., Zhang, S.H., and Guo, R.R., 2013. Geochemistry and zircon U–Pb–Hf isotopes of the late Paleoproterozoic Jianping diorite–monzonite–syenite suite of the North China Craton: Implications for petrogenesis and geodynamic setting. *Lithos*, 162–163: 175–194.
- Wang W.Q., Xu Z.Y., Liu Z.H., Zhao Q.Y. and Jiang X.J., 2013. Early-Middle Permian tectonic evolution of the central-northern margin of the North China Craton: Constraints from zircon U–Pb ages and geochemistry of the granitoids. *Acta Petrologica Sinica*, 29(9): 2987–3003 (in Chinese with English abstract).
- Wang, X., Li, X.P., and Han, Z.Z., 2018. Zircon ages and geochemistry of amphibolitic rocks from the Paleoproterozoic Erdaowa Group in the Khondalite Belt, North China Craton and their tectonic implications. *Precambrian Research*, 317: 253–267.
- Wang, X.X., Wang, T., Castro, A., Ke, C.H., Yang, Y., and Hu, N.G., 2018. Magmatic evolution and source of a Proterozoic rapakivi granite complex in the North China Craton: New evidence from zircon U–Pb ages, mineral compositions, and geochemistry. *Journal of Asian Earth Sciences*, 167: 165–180.
- Wang, Y.J., Fan, W.M., Zhang, Y.H., Guo, F., Zhang, H.F., and Peng, T.P., 2004. Geochemical, $^{40}\text{Ar}/^{39}\text{Ar}$ geochronological and Sr–Nd isotopic constraints on the origin of Paleoproterozoic mafic dykes from the southern Taihang Mountains and implications for the ca. 1800Ma event of the North China Craton. *Precambrian Research*, 135(1): 55–77.
- Wen, B., Evans, D.A.D., Wang, C., Li, Y.X., and Jing, X.Q., 2018. A positive test for the Greater Tarim Block at the heart of Rodinia: Mega–dextral suturing of supercontinent assembly. *Geology*, 46(8): 687–690.
- Whitehouse, M.J., and Platt, J.P., 2003. Dating high–grade metamorphism—constraints from rare–earth elements in zircon and garnet. *Contributions to Mineralogy and Petrology*, 145(1): 61–74.
- Wingate, M.T.D., Pisarevsky, S.A., and Evans, D.A.D., 2002. Rodinia connections between Australia and Laurentia: no SWEAT, no AUSWUS? *Terra Nova*, 14(2): 121–128.
- Won Kim, S., Kwon, S., Santosh, M., Cho, D.L., Kee, W.S., Lee, S.B., and Jeong, Y.J., 2019. Detrital zircon U–Pb and Hf isotope characteristics of the Early Neoproterozoic successions in the central–western Korean Peninsula: Implication for the Precambrian tectonic history of East Asia. *Precambrian Research*, 322: 24–41.
- Xia, X.P., Sun, M., Zhao, G.C., and Luo, Y., 2006. LA–ICP–MS U–Pb geochronology of detrital zircons from the Jining Complex, North China Craton and its tectonic significance. *Precambrian Research*, 144(3–4): 199–212.
- Xiao, W.J., Windley, B.F., Hao, J., and Zhai, M.G., 2003. Accretion leading to collision and the Permian Solonker suture, Inner Mongolia, China: Termination of the central Asian orogenic belt. *Tectonics*, 22(6): 1609, <http://dx.doi.org/10.1029/2002TC001484>.
- Xu, H.R., Yang, Z.Y., Peng, P., Meert, J.G., and Zhu, R.X., 2014. Paleo–position of the North China craton within the supercontinent Columbia: Constraints from new paleomagnetic results. *Precambrian Research*, 255, 276–293.
- Xu, Z.Y., Wan, Y.S., Dung, C.Y., and Ma, M.Z., 2015. Late Neoproterozoic magmatism identified in Daqingshan, Inner Mongolia: SHRIMP zircon U–Pb dating. *Acta Petrologica Sinica*, 31(6): 1509–1517 (in Chinese with English abstract).
- Yang, J.H., Wu, F.Y., Liu, X.M., and Xie, L.W., 2005. Zircon U–Pb ages and Hf isotopes and their geological significance of the Miyun rapakivi granites from Beijing, China. *Acta Petrologica Sinica*, 21(6): 1633–1644 (in Chinese with English abstract).
- Yang, K.F., Fan, H.R., Santosh, M., Hu, F.F., and Wang, K.Y., 2011. Mesoproterozoic carbonatitic magmatism in the Bayan Obo deposit, Inner Mongolia, North China: Constraints for the mechanism of super accumulation of rare earth elements. *Ore Geology Reviews*, 40(1): 122–131.
- Yang, K.F., Fan, H.R., Hu, F.F., and Wang, K.Y., 2012. Sediment source of Bayan Obo marginal rift and genesis of ore–bearing dolomite of the giant REE deposit. *Acta Geologica Sinica (English Edition)*, 86(5): 775–784 (in Chinese with English abstract).
- Yuan, H.L., Gao, S., Liu, X.M., Li, H.M., Günther, D., and Wu, F.Y., 2004. Accurate U–Pb Age and Trace Element Determinations of Zircon by Laser Ablation–Inductively Coupled Plasma–Mass Spectrometry. *Geostandards and Geoanalytical Research*, 28(3): 353–370.
- Zhai, M.G., and Liu, W., 2003. Palaeoproterozoic tectonic history of the North China craton: a review. *Precambrian Research*, 122(1): 183–199.
- Zhai, M.G., and Santosh, M., 2011a. The early Precambrian odyssey of the North China Craton: A synoptic overview. *Gondwana Research*, 20(1): 6–25.
- Zhai, M.G., 2011b. Cratonization and the Ancient North China Continent: A summary and review. *Science China Earth Sciences*, 54(8): 1110 (in Chinese with English abstract).
- Zhai, M.G., 2013. The main old lands in China and assembly of Chinese unified continent. *Science China Earth Sciences*, 56(11): 1829–1852 (in Chinese with English abstract).
- Zhai, M.G., 2014. Multi–stage crustal growth and cratonization of the North China Craton. *Geoscience Frontiers*, 5(4): 457–469 (in Chinese with English abstract).
- Zhai, M.G., Hu, B., Zhao, T.P., Peng, P., and Meng, Q.R., 2015. Late Paleoproterozoic–Neoproterozoic multi–rifting events in the North China Craton and their geological significance: A study advance and review. *Tectonophysics*, 662: 153–166.
- Zhang, S.H., Liu, S.W., Zhao, Y., Yang, J.H., Song, B., and Liu, X.M., 2007. The 1.75–1.68Ga anorthosite–mangerite–alkali granitoid–rapakivi granite suite from the northern North China Craton: Magmatism related to a Paleoproterozoic orogen. *Precambrian Research*, 155(3): 287–312.
- Zhang, S.H., Zhao, Y., Yang, Z.Y., He, Z.F., and Wu, H., 2009. The 1.35Ga diabase sills from the northern North China Craton: Implications for breakup of the Columbia (Nuna) supercontinent. *Earth and Planetary Science Letters*, 288(3): 588–600.
- Zhang, S.H., Zhao, Y., and Santosh, M., 2012. Mid–Mesoproterozoic bimodal magmatic rocks in the northern North China Craton: Implications for magmatism related to breakup of the Columbia supercontinent. *Precambrian Research*, 222–223: 339–367.
- Zhang, S.H., Zhao, Y., Li, X.H., Ernst, R.E., and Yang, Z.Y., 2017. The 1.33–1.30 Ga Yanliao large igneous province in the North China Craton: Implications for reconstruction of the Nuna (Columbia) supercontinent, and specifically with the North Australian Craton. *Earth and Planetary Science Letters*, 465: 112–125.
- Zhang, S.H., Li, Z.X., and Wu, H.C., 2006. New Precambrian palaeomagnetic constraints on the position of the North China Block in Rodinia. *Precambrian Research*, 144(3): 213–238.
- Zhang, S.H., Li, Z.X., Evans, D.A.D., Wu, H.C., Li, H.Y., and Dong, J., 2012. Pre–Rodinia supercontinent Nuna shaping up: A global synthesis with new paleomagnetic results from North China. *Earth and Planetary Science Letters*, 353–354: 145–155.
- Zhang, S.H., Zhao, Y., Ye, H., and Hu, J.M., 2013. New constraints on ages of the Chuanlinggou and Tuanshanzi formations of the Changcheng System in the Yan–Liao area in the northern North China Craton. *Acta Petrologica Sinica*, 29(7): 2481–2490 (in Chinese with English abstract).
- Zhang, X.H., Yuan, L.L., Xue, F.H., and Zhai, M.G., 2014. Neoproterozoic metagabbro and charnockite in the Yinshan

- Block, western North China Craton: Petrogenesis and tectonic implications. *Precambrian Research*, 255: 563–582.
- Zhang, X., 2014. Thrusting Folds to the North of the Giant Bayan Obo Ore Deposit. China University of Petroleum (East China) (Master Thesis): 1-91 (in Chinese with English abstract).
- Zhao, G.C., Cawood, P., and Lu, L.Z., 1999a. Petrology and P–T history of the Wutai amphibolites: implications for tectonic evolution of the Wutai Complex, China. *Precambrian Research*, 93(2-3): 181–199.
- Zhao, G.C., Wilde, S.A., Cawood, P.A., and Lu, L.Z., 1999b. Tectonothermal history of the basement rocks in the western zone of the North China Craton and its tectonic implications. *Tectonophysics*, 310(1-4): 37–53.
- Zhao, G.C., Cawood, P.A., Wilde, S.A., Min, S., and Lu, L.Z., 2000a. Metamorphism of basement rocks in the Central Zone of the North China Craton: implications for Paleoproterozoic tectonic evolution. *Precambrian Research*, 103(1-2): 55–88.
- Zhao, G.C., Wilde, S.A., Cawood, P.A., and Lu, L.Z., 2000b. Petrology and P–T path of the Fuping mafic granulites: implications for tectonic evolution of the central zone of the North China Craton. *Journal of Metamorphic Geology*, 18(4): 375–391.
- Zhao, G.C., Sun, M., Wilde, S.A., and Li, S.Z., 2003. Assembly, Accretion and Breakup of the Paleo– Mesoproterozoic Columbia Supercontinent: Records in the North China Craton. *Gondwana Research*, 6(3): 417–434.
- Zhao, G.C., Sun, M., Wilde, S.A., and Li, S.Z., 2004. A Paleo–Mesoproterozoic supercontinent: assembly, growth and breakup. *Earth-Science Reviews*, 67(1): 91–123.
- Zhao, G.C., Sun, M., Wilde, S.A., Li, S.Z., Liu, S.W., and Zhang, J., 2006. Composite nature of the North China Granulite–Facies Belt: Tectonothermal and geochronological constraints. *Gondwana Research*, 9(3): 337–348.
- Zhao, G.C., Wilde, S.A., Sun, M., Li, S.Z., Li, X.P., and Zhang, J., 2008. SHRIMP U–Pb zircon ages of granitoid rocks in the Lüliang Complex: Implications for the accretion and evolution of the Trans–North China Orogen. *Precambrian Research*, 160(3): 213–226.
- Zhao, G.C., Li, S.Z., Sun, M., and Wilde, S.A., 2011. Assembly, accretion, and break-up of the Palaeo– Mesoproterozoic Columbia supercontinent: record in the North China Craton revisited. *International Geology Review*, 53(11-12): 1331–1356.
- Zhao, G.C., Cawood, P.A., Li, S.Z., Wilde, S.A., Sun, M., Zhang, J., He, Y.H., and Yin, C.Q., 2012. Amalgamation of the North China Craton: Key issues and discussion. *Precambrian Research*, 222–223: 55–76.
- Zhao, T.P., Jin, C.W., Zhai, M.G., Xia, B., and Zhou, M.F., 2002. Geochemistry and petrogenesis of the Xiong'er Group in the southern regions of the North China Craton. *Acta Petrologica Sinica*, 18(1): 59–69 (in Chinese with English abstract).
- Zhao, T.P., Chen, F.K., Zhai, M.G., Xia, B., 2004a. Single zircon U–Pb ages and their geological significance of the Damiao anorthosite complex, Hebei Province, China. *Acta Petrologica Sinica*, 20(3): 685–690 (in Chinese with English abstract).
- Zhao, T.P., Zhai, M.G., Xia, B., Li, H.M., Zhang, Y.X., and Wan, Y.S., 2004b. Zircon U–Pb SHRIMP dating for the volcanic rocks of the Xiong'er Group: Constraints on the initial formation age of the cover of the North China Craton. *Chinese Science Bulletin*, 49(23): 2495–2502 (in Chinese with English abstract).
- Zhong, Y., Zhai, M.G., Peng, P., Santosh, M., and Ma, X.D., 2015. Detrital zircon U–Pb dating and whole-rock geochemistry from the clastic rocks in the northern marginal basin of the North China Craton: Constraints on depositional age and provenance of the Bayan Obo Group. *Precambrian Research*, 258: 133–145.
- Zhou, Z.G., Wang, G.S., Zhang, D., and Gu, Y.C., 2016. Zircon ages of gabbros in the Siziwangqi, Inner Mongolia and its constrain on the formation time of the Bayan Obo Group. *Acta Petrologica Sinica*, 32(6): 1809–1822 (in Chinese with English abstract).
- Zhou, Z.G., Hu, M.M., Wu, C., Wang, G.S., Liu, C.F., Cai, A., and Jiang, T., 2018. Coupled U–Pb dating and Hf isotopic analysis of detrital zircons from Bayan Obo Group in Inner Mongolia: Constraints on the evolution of the Bayan Obo rift belt. *Geological Journal*, 53(6): 2649–2664.

About the first author



LI Changhai, Male, born in 1993 in Dongying City, Shandong Province; a master student in College of the Earth Sciences, Jilin University, my research interests mainly lie in Precambrian geology and supercontinent reconstruction, Email: changhai0912@163.com, Phone: 13144315168.

About the corresponding author



LIU Zhenghong, Male, born in 1960 in Dandong City, Liaoning Province; professor in College of the Earth Sciences, Jilin University, he is now interested in the study of structural analysis, Email: liuzh@jlu.edu.cn, Phone: 18686680810.